

TABLE OF CONTENTS

	<u>Page</u>
ABSTRACT	
ACKNOWLEDGMENTS	ii 1/A4
TABLE OF CONTENTS	iii 1/A5
LIST OF TABLES	iv 1/A6
LIST OF FIGURES	v 1/A7
NOTATION	vi 1/A8
INTRODUCTION	1 1/A12
THE EXPERIMENT	8 1/B5
I. IN-FLIGHT SIMULATION	8 1/B5
II. AIRCRAFT CONFIGURATIONS	9 1/B6
III. DATA COLLECTION	10 1/B7
CLOSED LOOP ANALYSIS	11 1/B8
RESULTS AND DISCUSSION	15 1/B12
I. PILOT TECHNIQUE	15 1/B12
II. EFFECT OF THROTTLE LAG	18 1/C1
III. EFFECT OF TURBULENCE	20 1/C3
IV. EFFECT OF SAS GAIN	21 1/C4
V. LOAD FACTOR IN THE FLARE	22 1/C5
VI. EFFECT OF $Z_{\delta T}$ INCREASE	25 1/C8
VII. RATE COMMAND VS ATTITUDE COMMAND	25 1/C8
SUGGESTIONS FOR FURTHER RESEARCH	26 1/C9
CONCLUSIONS	29 1/C12
REFERENCES	30 1/C13

Item 830-H-14

NAS 1.26: 3191

DEC 28 1979

NASA Contractor Report 3191

COMPLETED

ORIGINAL

An Exploratory Investigation of the STOL Landing Maneuver

Patrick H. Whyte

**CONTRACT NAS2-7350
DECEMBER 1979**

NASA

74

NASA Contractor Report 3191

An Exploratory Investigation of the STOL Landing Maneuver

Patrick H. Whyte
Princeton University
Princeton, New Jersey

Prepared for
Ames Research Center
under Contract NAS2-7350



National Aeronautics
and Space Administration

Scientific and Technical
Information Branch

1979

ACKNOWLEDGMENTS

The evaluation pilots, Mr. David R. Ellis and Mr. Roger H. Hoh, were indispensable both for their tireless flying and for their guidance during many fruitful discussions. Professor Edward Seckel, who contributed to several of these discussions, is deserving of mention as well. To the Hangar staff and the safety pilot I also express my gratitude for their assistance.

My thanks go out to Mrs. Grace Arnesen for her typing of this report and to Miss Louise Schaufler, who prepared the figures.

This thesis carries number 1231-T in the records of the Department of Aerospace and Mechanical Sciences.

TABLE OF CONTENTS

	<u>Page</u>
ABSTRACT	
ACKNOWLEDGMENTS	ii
TABLE OF CONTENTS	iii
LIST OF TABLES	iv
LIST OF FIGURES	v
NOTATION	vi
INTRODUCTION	1
THE EXPERIMENT	8
I. IN-FLIGHT SIMULATION	8
II. AIRCRAFT CONFIGURATIONS	9
III. DATA COLLECTION	10
CLOSED LOOP ANALYSIS	11
RESULTS AND DISCUSSION	15
I. PILOT TECHNIQUE	15
II. EFFECT OF THROTTLE LAG	18
III. EFFECT OF TURBULENCE	20
IV. EFFECT OF SAS GAIN	21
V. LOAD FACTOR IN THE FLARE	22
VI. EFFECT OF $Z_{\delta T}$ INCREASE	25
VII. RATE COMMAND VS ATTITUDE COMMAND	25
SUGGESTIONS FOR FURTHER RESEARCH	26
CONCLUSIONS	29
REFERENCES	30

LIST OF TABLES

	<u>Page</u>
I. OPEN LOOP TRANSFER FUNCTIONS	32
II. STABILITY DERIVATIVES	33
III. CLOSED LOOP TRANSFER FUNCTIONS	34
IV. LANDING DATA	35
V. PILOT RATINGS AND COMMENTARY	38

LIST OF FIGURES

- Figure 1. Examples of Time Response Characteristics
- Figure 2. Typical Flight Path and Airspeed Response to Control Inputs, $d\gamma/dV > 0$
- Figure 3. Examples of Steady-State V - γ - θ plots
- Figure 4. Parameter Definition, Step Throttle Input
- Figure 5. Configuration Values of $(\frac{\Delta\gamma_{max}}{\Delta\gamma_{ss}})_{\Delta T}$, $(\frac{\Delta V_{ss}}{\Delta\gamma_{ss}})_{\Delta T}$, τ_γ , Z_w , and $d\gamma/dV$
- Figure 6. STOL Runway Setup
- Figure 7a. Rate Command/ Attitude Hold SAS
- Figure 7b. Attitude Command/ Attitude Hold SAS
- Figure 8. Typical Landing Results for Each Configuration
- Figure 9. Closed Loop Responses for TG- Aircraft
- Figure 10. BSL1 and AP1 Closed Loop Responses, Low Gain SAS, no Parallel Integrator or Actuator Lag
- Figure 11. BSL1 and AP1 Closed Loop Responses, Complete SAS, Low Gain
- Figure 12. BSL1 and AP1 Closed Loop Responses, Complete SAS, High Gain
- Figure 13. Effect of $d\gamma/dV$ and Z_w on Stick Response
- Figure 14. Possible Pilot Opinion Contours in the $Z_w - \frac{d\gamma}{dV}$ Plane
- Figure 15. Pilot Rating vs $\overline{\Delta n}$ for Some of the Configurations Tested
- Figure 16. Typical h - γ Trajectories for Several Configurations

NOTATION

$()_o$	approach condition
$()_i$	condition at flare initiation point
$()_{TD}$	touchdown condition
$(\dot{})$	rate of change with respect to time
$()_c$	command variable
$()'$	closed loop root (s)
$()_{\theta-\delta_e}$	closed loop transfer function
V	airspeed (knots or feet/sec)
h	altitude (feet)
α	angle of attack (radians)
θ	pitch attitude (degrees or radians)
γ	flight path angle (degrees or radians)
q	pitch rate $\dot{\theta}$ (rad/sec)
δ_e	elevator deflection (radians)
δ_T	throttle displacement (mm)
δ_s	stick deflection (inches)
Z_α	heave damping (ft/sec ² /rad)
Z_w	Z_α / V_o (/sec-rad)
X_α	induced drag (ft/sec ² /rad)
X_w	X_α / V_o (/sec-rad)

M_{α}	angle of attack stability (/ sec ²)
$M_{\dot{\alpha}}$	angle of attack damping (/ sec)
Z_u	normal acceleration due to speed change (/ sec)
X_u	drag damping (/ sec)
M_u	speed stability (ft/ sec)
M_q	pitch damping (/ sec)
Z_{δ_e}	normal acceleration due to elevator deflection (ft/ sec ² / rad)
M_{δ_e}	longitudinal control sensitivity (/ sec ²)
Z_{δ_T}	normal acceleration due to throttle displacement (ft/ sec ² / mm)
X_{δ_T}	forward acceleration due to throttle displacement (ft/ sec ² / mm)
M_{δ_T}	angular acceleration due to throttle displacement (/ sec ² -mm)
K_{θ}	pitch attitude feedback gain to elevator (deg/ deg)
$K_{\dot{\theta}}$	pitch rate feedback gain to elevator (deg/ deg/ sec)
K_I	gain of pitch rate command integrator (deg/ sec/ deg)
K_{δ}	stick position feed forward gain (deg/ inch)
g	acceleration due to gravity (ft/ sec ²)
s	Laplace variable
Δ_L	open loop longitudinal denominator
N_i^r	numerator of the transfer function relating response r to input i
$N_{\delta_e \delta_T}^{\theta \gamma}$	coupling numerator for flight path response to thrust with attitude to elevator loop closed

ζ_p, ω_p	damping ratio and natural frequency (rad/sec) of the phugoid mode
$\zeta_\theta, \omega_\theta$	damping ratio and natural frequency (rad/sec) of the numerator roots of the attitude to elevator transfer function
$\frac{1}{T_{\theta_1}}, \frac{1}{T_{\theta_2}}$	real roots of the numerator of the attitude to elevator transfer function (/ sec)
$\frac{1}{T_{sp_1}}, \frac{1}{T_{sp_2}}$	real roots of the short period mode (/ sec)
$\frac{1}{T_{L\theta}}$	$K_\theta / K_{\dot{\theta}}$ (/ sec)
$\frac{1}{T_{\gamma_1}}, \frac{1}{T_{\gamma_2}}, \frac{1}{T_{\gamma_3}}$	real roots of the numerator of the flight path to elevator transfer function (/ sec)
$\frac{1}{T_{\gamma T_1}}, \frac{1}{T_{\gamma T_2}}, \frac{1}{T_{\gamma T_3}}$	real roots of the numerator of the flight path to throttle transfer function (/ sec)
$\frac{1}{T_{\gamma T}}$	root of $N_{\delta_e}^{\theta} \delta_T^{\gamma}$ (/ sec)
$\frac{1}{T_{u_1}}$	low frequency root of the numerator of the airspeed to attitude transfer function
$\frac{1}{T_{uT}}$	low frequency root of the numerator of the thrust to airspeed transfer function, attitude loop closed
$A_{\gamma\theta}$	gain of the flight path to attitude transfer function
$A_{\gamma T}$	gain of the flight path to thrust transfer function
$A_{\theta\gamma}$	gain of the attitude to flight path transfer function
$A_{u\theta}$	gain of the airspeed to attitude transfer function

A_{uT}	gain of the airspeed to thrust transfer function
Y_{θ}	$K_{\dot{\theta}} s + K_{\theta}$ (deg/deg)
a	parallel integrator gain (/ sec)
Δt	time required to flare aircraft (sec)
$\overline{\Delta n}$	average load factor generated in the flare (g)
w_g	vertical turbulence component (ft/sec)
u_g	longitudinal turbulence component (ft/sec)
σ_u	root mean square u_g turbulence velocity (ft/sec)
τ_T	first order throttle lag time constant (sec)
τ_e	actuator lag (sec)
τ_{γ}	time constant of initial flight path response to thrust (sec)
$\frac{d\gamma}{dV}$	backsidedness parameter (deg/knot)
$\left(\frac{\Delta V_{ss}}{\Delta \gamma_{ss} \Delta T}\right)$	ratio of change of steady-state airspeed to flight path due to a thrust change, θ constant (kt/deg)
$\left(\frac{\Delta \gamma_{max}}{\Delta \gamma_{ss} \Delta T}\right)$	ratio of maximum to steady-state change of flight path due to a change in thrust, θ constant
$ $	absolute value
Δ	incremental value

INTRODUCTION

Transport category aircraft of the Short Takeoff and Landing (STOL) variety are required, in the course of their mission, to make steep approaches to the landing field at speeds normally associated with small, conventional, general aviation aircraft. Because a significant amount of power is used to supplement the basic aerodynamics of the vehicle in the approach configuration, manual control is generally more difficult than control of a conventional transport aircraft operating at higher speeds. As indicated in Reference 1, use of conventional controls such as elevator or throttle is likely to produce rather unconventional behavior as a result of:

- sluggish pitch-attitude response and strong excitation of the phugoid mode;
- sluggish flight path response to attitude changes;
- operation on the back side of the thrust-required curve;
- large changes in lift and drag with engine power setting;
- significant coupling between flight path and airspeed with either attitude or power changes.

The longitudinal handling qualities are degraded to the extent that some sort of stability augmentation system (SAS) is usually necessary; attitude must be controlled tightly in order for the pilot to attain precise control over flight path and airspeed. When attitude may be assumed constant, the resulting closed loop aircraft responses to stick and throttle inputs are as follows:

$$\left(\frac{\gamma}{\theta_c}\right)_{\theta \rightarrow \delta e} = \frac{A_{\gamma\theta} \left(s + \frac{1}{T_{\gamma_1}}\right)}{s^2 + 2\zeta_{\theta} \omega_{\theta} s + \omega_{\theta}^2}$$

$$\left(\frac{u}{\theta_c}\right)_{\theta \rightarrow \delta e} = \frac{A_{u\theta} \left(s + \frac{1}{T_{u_1}}\right)}{s^2 + 2\zeta_{\theta} \omega_{\theta} s + \omega_{\theta}^2}$$

$$\left(\frac{y}{\delta_T}\right)_{\theta \rightarrow 0} = \frac{A_{y_T} \left(s + \frac{1}{T_{y_T}}\right)}{s^2 + 2\zeta_{\theta} \omega_{\theta} s + \omega_{\theta}^2}$$

$$\left(\frac{u}{\delta_T}\right)_{\theta \rightarrow 0} = \frac{A_{u_T} \left(s + \frac{1}{T_{u_T}}\right)}{s^2 + 2\zeta_{\theta} \omega_{\theta} s + \omega_{\theta}^2}$$

These path and speed transfer functions to attitude and thrust all appear in the general form

$$\frac{\text{response}}{\text{command}} = \frac{A \left(s + \frac{1}{T}\right)}{s^2 + 2\zeta_{\theta} \omega_{\theta} s + \omega_{\theta}^2}$$

The variables involved are the gain A , the numerator root $1/T$, and the denominator values of ζ_{θ} and ω_{θ} (or $1/T_{\theta_1}$ and $1/T_{\theta_2}$). The correspondence between these features and a time history of the response is indicated in Figure 1, adapted from Reference 6.

Since $2\zeta_{\theta} \omega_{\theta} \doteq -Z_w - X_u$ and $\omega_{\theta}^2 \doteq Z_w X_u - Z_u X_w$, it is apparent that the characteristic modes of the closed loop system are defined by the basic aircraft lift and drag terms, Z_w and X_u , plus the coupling terms X_w and Z_u . These latter two are responsible for the degree of coupling between the speed and flight path modes. When their product $X_w Z_u$ is large and negative the modes are oscillatory and when their product is small the modes are two first order subsidences. Because the control input transfer function numerators are all first order, there can be no true cancellation of (selective) poles and zeros when the modes are oscillatory. The result is that speed and flight path motions occur with the same dynamics and are inherently coupled. Fortunately, the modes are often two first order subsidences well separated in frequency. Then, as Reference 2 points out, the path and speed responses may be well separated in frequency and hence easier to control independently.

As noted above, both pitch attitude and thrust can significantly affect flight path and airspeed response. Different techniques may be hypothesized regarding the manner in which the pilot utilizes these controls. Figure 2 presents typical STOL behavior in response to stick and throttle inputs. These time histories correspond to particular cases of Figure 1. The response to an attitude change at constant thrust is shown in Figure 2(a) for an aircraft on the back side of the power curve. For a nose-up attitude change, flight path initially shallows but eventually steepens so that attitude control of flight path is poor in the approach and landing situation. Airspeed response is conventional, suggesting that speed control with attitude is satisfactory. When thrust is increased at constant attitude, as displayed in Figure 2(b), flight path responds quickly, with the long term change determined by specific configuration characteristics. Speed, on the other hand, is reduced, making the throttle a poor speed control. The pilot may then be expected to use attitude to control airspeed and thrust to control flight path.

A plot of flight path vs airspeed (V - γ) contours for constant power settings and pitch attitudes is most useful for examining the steady-state performance characteristics discussed above in regard to Figure 2. As pointed out in Reference 7, such a map graphically shows how the steady-state values of the important responses vary with trim condition. Figure 3 displays the aforementioned contours for two configurations which will be of interest later in the report. The slope $d\gamma/dV$ of the constant power lines, known as the back-sidedness parameter, defines the appropriate control technique for the pilot. Values of $d\gamma/dV > 0$ are associated with the back side of the curve. In this range a nose-up attitude change at constant power produces a steady-state steepening of the flight path and a decrease in airspeed. A throttle increase at constant attitude, for the aircraft displayed in Figure 3, results either in a speed increase or reduction, depending upon the configuration. These results are consistent with the time responses of Figure 2 and support the

contention that the pilot will control speed with attitude and flight path with throttle in the back side region.

The slope of the constant attitude lines, $(\Delta V_{ss} / \Delta \gamma_{ss})_{\Delta T}$, defines the steady-state flight path-airspeed coupling for the configuration. Positive values of this parameter are referred to as proverse coupling, meaning that for constant attitude flight the trim speed will increase as the flight path angle is increased with power. Proverse coupling is typical of conventional aircraft, while STOL vehicles may display strong adverse coupling as well. The spacing of the attitude lines along lines of constant speed is indicative of the pitch change required to hold airspeed constant while changing flight path with power. This gradient tends to become quite nonlinear at low power settings for adversely coupled vehicles.

Based on the time histories of responses to control inputs and on the steady-state properties of STOL aircraft, the following parameters, defined in Figure 4, have been introduced along with $d\gamma/dV$ and Z_w to characterize STOL behavior in the approach:

- i) τ_γ , the time constant of the flight path response;
- ii) $(\frac{\Delta \gamma_{max}}{\Delta \gamma_{ss}})_{\Delta T}$, the flight path overshoot; and
- iii) $(\frac{\Delta V_{ss}}{\Delta \gamma_{ss}})_{\Delta T}$, the flight path-airspeed coupling.

Research is currently being conducted at Princeton to explore some of the problems of flight path and airspeed control for the STOL approach and landing. The configurations investigated to date are listed in Table I, together with their open loop properties. *

* The transfer functions listed in Table I are derived from this approximate form of the equations of motion:

$$\begin{bmatrix} s - X_u & -X_\alpha & g \\ -Z_u/V_0 & s - Z_\alpha/V_0 & -s \\ -M_u & -M_\alpha - M_{\dot{\alpha}}s & s(s - M_q) \\ 0 & 1 & -1 \end{bmatrix} \begin{bmatrix} V \\ \alpha \\ \theta \\ \gamma \end{bmatrix} = \begin{bmatrix} 0 & X_{sT} \\ 0 & Z_{sT}/V_0 \\ M_{\delta_e} & M_{\delta_T} \\ 0 & 0 \end{bmatrix} \begin{bmatrix} \delta_e \\ \delta_T \end{bmatrix}$$

The first two configurations in Table I, called BSL1 and AP1, arose from an effort to identify the minimal acceptable characteristics for manual STOL flight path control (see Reference 7). For the purpose of that work, they are meant to represent marginal aircraft of a specific genre. BSL1 is a simulation of a low efficiency, externally blown jet flap STOL, while AP1 resembles a STOL employing a low efficiency vectored thrust-mechanical flap combination. The other configurations listed in Table I have been generated in order to supplement research under way at NASA's Ames Research Center with a modified DeHavilland of Canada C-8A "Buffalo" incorporating internally blown augmentor flaps and vectored jet thrust. As may be expected, these latter aircraft are significantly different in several aspects from BSL1 and AP1, coming as they do from another research program. These differences will be explored in an attempt to link the results of the two efforts.

Of the configurations in Table I, the following have been selected for detailed analysis in this report: BSL1, AP1, TG1A, TG4A, TG1C, and TG3C. Their stability derivatives are noted in Table II. In Figure 5, the various values of τ_γ , $(\frac{\Delta \gamma_{\max}}{\Delta \gamma_{ss}})_{\Delta T}$, $(\frac{\Delta V_{ss}}{\Delta \gamma_{ss}})_{\Delta T}$, Z_w , and $\frac{d\gamma}{dV}$ are indicated as well. Hopefully, the flight data from these six configurations will shed some light on the problems associated with the STOL landing maneuver, although the aircraft of Table I were basically designed for simulation of the approach condition. As the experimental results are readily available, their analysis makes a useful starting point; for future programs, configurations more appropriate for flare analysis may be generated.

Although the problem of the STOL approach has been actively addressed in recent years, the difficulties with the flare maneuver have yet to be deeply explored. Future research at Princeton will be progressing in this direction, and indeed an attempt has been made (Reference 3) to evaluate the landing capabilities of conventional aircraft. These landings were executed either with the stick alone or with the stick as the primary control with assistance from the

throttle as secondary control. For the two-control landing, two distinct pilot techniques were apparent from the experimental results.

The selection of one or the other of these techniques by the pilot is related to the amount of deceleration the airplane experiences in the flare. The linearized, constant-coefficient flare equations derived in Reference 3 express this deceleration as

$$\Delta V = \frac{\overline{\Delta n}}{\left(\frac{d\gamma}{dV}\right)^2} \left[\frac{1}{V_0} + K \frac{d\gamma}{dV} \right] \left[1 - \exp \left(V_0 \frac{d\gamma}{dV} \frac{\Delta \gamma}{\overline{\Delta n}} \right) \right] + \frac{\Delta \gamma}{\left(\frac{d\gamma}{dV}\right)}$$

where K is a parameter related to the lift and drag changes resulting from control actions.* From this equation it may be established that increasing $\Delta \gamma$ or $d\gamma/dV$, or decreasing V_0 or $\overline{\Delta n}$ causes increased deceleration in the flare.

Consider landings executed with the stick alone. The pilot of a conventional airplane prefers to touch down on the runway at a speed just above the stall speed of the aircraft. Since V_0 is usually about $1.3 V_{TD}$, there is a fixed amount of deceleration associated with a good flare. Assuming γ_0 is fixed, the pilot will then play $\overline{\Delta n}$ against $d\gamma/dV$ in order to acquire the proper amount of deceleration in the landing. A frontside vehicle, for which $d\gamma/dV < 0$, must be flared slowly at low $\overline{\Delta n}$, leading to long touchdown distances. Failure to do so will cause the aircraft to land "hot." On the other hand, backside aircraft experience a great deal of deceleration in the flare unless they are flared quickly, at a high load factor, in an attempt to prevent high touchdown sink rates.

Utilization of the throttle as a secondary control in the flare can alleviate these difficulties to some extent. A throttle reduction either prior to or during the flare counteracts the tendency of frontside airplanes to float a long distance down the runway before touchdown. The use of the throttle in this manner is described by the term "decelerate technique." This is the technique most

* The actual value of K is of little significance here, except to say that $K > 0$ for the aircraft discussed in Reference 3.

avored by pilots, since wheel and throttle actions may be well coordinated, working in a sense like some equivalent single control. Conversely, to counteract the effect of excess deceleration in the flare the pilot employs the "accelerate technique" in which power is added through the flare to supplement the stick action and produce softer touchdowns. Pilots find this method to be somewhat more difficult and demanding, as stick and throttle movements are opposite in direction, leading to poor coordination and inconsistent landings.

This report is intended to extend the discussion of the landing maneuver to the case of STOL aircraft. The powered lift capability of these vehicles introduces another degree of freedom into the landing analysis: it becomes feasible to flare the aircraft using the throttle as the primary control. The resulting modification to the pilot technique is explored in later sections and attempts are made to link pilot opinion rating to the relevant parameters.

THE EXPERIMENT

I. IN-FLIGHT SIMULATION:

The Princeton variable stability Navion, N5113K (Reference 4) was used to simulate the chosen configurations. An analog computer matching technique was used to verify the accuracy of the simulation; that is, the aircraft and computer responses were compared for the same control inputs and the appropriate airplane feedbacks were adjusted to obtain proper matching in terms of frequency, amplitude, time constant, and general shape.

The experimental landings were executed in touch-and-go style in calm air. On final approach, the safety pilot acquired the 6° glideslope, trimmed the airplane at the relevant speed, and turned over command to the evaluation pilot for the last 600-800 ft, or 15-20 seconds, of the approach. The approach speeds were 70 kt for the TG-aircraft and 75 kt for BSL1 and AP1. Glide slope tracking was achieved by means of a TALAR MLS unit and an optical glide slope light system, located as shown in Figure 6. At the end of the approach, the evaluation pilot attempted to flare and land the vehicle in the STOL zone. Two evaluation pilots were employed in the program. Pilot 2 flew all six configurations, while Pilot 1 flew BSL1 and AP1 only.

To perceive the effect of turbulence on the landing maneuver, BSL1 and AP1 were flown in calm air and at two levels of simulated turbulence, the rms u-component gust velocities in each case being $\sigma_u = 0, 2.25, \text{ and } 4.5 \text{ ft/sec}$. Only longitudinal gusts (u_g) and vertical gusts (w_g) were programmed into the aircraft. The w_g rms velocities were about fifty percent smaller than σ_u ; w_g was scaled for an altitude of 200 ft. Since real vertical turbulence components are inversely proportional to altitude, this value of w_g was chosen as a compromise. The TG-configurations were flown with no simulated turbulence.

Lift and moment ground effects of the basic Navion were cancelled by appropriate feedbacks from the radar altimeter. The details of this procedure may be found in Reference 8.

II. AIRCRAFT CONFIGURATIONS:

As mentioned above, the TG-configurations were generated to supplement a NASA-Ames program which explored variations in τ_y , $(\frac{\Delta V_{ss}}{\Delta y_{ss}}) \Delta T$, $(\frac{\Delta y_{max}}{\Delta y_{ss}}) \Delta T$ and their effect on handling qualities. Consequently, the longitudinal stability derivatives were chosen to satisfy these given criteria. A procedure was developed on the analog computer for obtaining the values of these derivatives; it is described in Reference 5. The longitudinal handling qualities were improved by means of the tight rate command/ attitude hold SAS depicted in Figure 7a.

Stability augmentation for BSL1 and AP1 took the form of the attitude command/ attitude hold SAS of Figure 7b. Two values of SAS gain were investigated for these aircraft. Because the feedbacks K_θ and $K_{\dot{\theta}}$ are mechanized through the elevator, and $M_{\delta e}$ varies between configurations, one must consider the products $K_\theta M_{\delta e}$ and $K_{\dot{\theta}} M_{\delta e}$ to compare the relative tightness of the SAS's involved:

	$K_\theta M_{\delta e}$	$K_{\dot{\theta}} M_{\delta e}$
BSL1, AP1 low gain	0.70	1.41
BSL1, AP1 high gain	1.75	1.75
TG-	2.40	2.40

The low gain BSL1-AP1 closure is loosest of all and is meant to be sluggish in response to commands. At high gain the behavior is greatly improved but it is not as snappy and tight as for the TG-airplanes.

Another discrepancy between configurations existed with respect to the throttle response. Most of the landings with BSL1 and AP1 were performed

when the throttle was equipped with a first order lag of time constant $\tau_T = 1.5$ sec. The other configurations incorporated a second order throttle lag of such damping and frequency as to resemble an "equivalent" first order lag of 0.4 sec. A few landings with BSL1 and AP1 were made with a first order lag of $\tau_T = 0.4$ sec for comparison.

The longitudinal equations of motion, as characterized by the longitudinal stability derivatives, are of more interest with respect to the flare maneuver than the lateral-directional equations. The lateral-directional derivatives were considered, however, to the extent that the lateral-directional handling qualities were made typical of large STOL transports, but augmented well enough so that they would not adversely influence the pilots' tasks of approach and landing.

III. DATA COLLECTION:

For each configuration, the pilots were requested to supply a Cooper-Harper pilot opinion rating for the approach condition and a separate rating for the flare and touchdown, both supplemented by appropriate commentary. Their comments and ratings for the flare maneuver are summarized in Table V.

During the flare, the aircraft motion variables were telemetered to the ground and recorded on magnetic tape for playback and analysis. Summaries of the landing results are presented in Table IV; typical flares with each airplane are displayed in Figure 8. The instant of touchdown was accurately identified by the spike in the landing gear strut accelerometer trace. The flare initiation point was identified by means of the \dot{h} trace and, depending on the pilot technique, the stick or throttle trace. This gave Δt , the time required for the flare, from which an average load factor in the flare was calculated according to

$$\Delta n = \frac{\dot{h}_i - \dot{h}_{TD}}{g \Delta t}$$

CLOSED LOOP ANALYSIS

Both evaluation pilots maintain that they exerted no conscious closed loop control over airspeed during the flare maneuver. Flight path control is the important consideration. The ability to control the airplane's path through space is dependent upon the closed loop properties of the vehicle as represented by θ/θ_c , $(\gamma/\theta_c)_{\theta \rightarrow \delta e}$ and $(\gamma/\delta T)_{\theta \rightarrow \delta e}$. These transfer functions are plotted in Figure 9 for the TG-aircraft. *

The θ/θ_c response is quite flat up to a frequency of about 1 rad/sec in all instances, as expected from the tightness of the SAS. As seen from the inset root loci accompanying Figure 9, the good response results from ω_p' being driven very close to the numerator zeros or, when $1/T_{\theta_2}$ is large, being driven out to a high frequency and damping. The root $1/T_{s_{p_1}}'$, also moves well to the left except for TG1A and TG1C, when it moves in close to $1/T_{\theta_1}$. This sort of behavior is very similar to that discussed in Reference 6, where "the compensation provided by Y_θ is intended to produce K/S characteristics in the crossover region for the attitude transfer function. It is apparent that both the short period and phugoid mode damping are increased and that the bandwidth of the system is extended to higher frequencies than for the open loop response." As indicated in Reference 6, the high gain of the SAS makes the closed loop approximation $\Delta_L' \doteq Y_\theta N_{\delta e}^\theta$ valid, so that

$$\left(\frac{\gamma}{\theta_c}\right)_{\theta \rightarrow \delta e} \doteq \frac{A_{\gamma_\theta} (s + T_{\gamma_1})}{[\zeta_\theta; \omega_\theta]}$$

$$\left(\frac{\gamma}{\delta T}\right)_{\theta \rightarrow \delta e} \doteq \frac{A_{\gamma_T} (s + \frac{1}{T_{\gamma_T}})}{[\zeta_\theta; \omega_\theta]}$$

These approximations are also plotted in Figure 9, where the latter approximation is seen to be excellent when compared to the derived transfer function. The

* The closed loop transfer functions for all aircraft investigated are catalogued in Table III.

former approximation varies somewhat in gain and general shape from the transfer function derived from the given equations of motion.

The discrepancy in shape between the derived and approximate $(\gamma/\theta_c)_{\theta \rightarrow \delta e}$ frequency responses is a consequence of neglecting the $Z_{\delta e}$ derivative in the equations of motion. The closed loop numerator for this transfer function is usually expressed as

$$N_{\delta e}^{\gamma} = A_{\gamma\theta} \left(s + \frac{1}{T_{\gamma_1}}\right) \left(s + \frac{1}{T_{\gamma_2}}\right) \left(s + \frac{1}{T_{\gamma_3}}\right)$$

Omitting $Z_{\delta e}$ eliminates the two high frequency zeros from this expression, leaving $1/T_{\gamma_1}$ only, so that the approximate and derived transfer functions diverge at high frequency. From a practical point of view, however, any poles or zeros located beyond the SAS bandwidth will have no appreciable effect on the handling qualities.

The difference in DC gains between the two $(\gamma/\theta_c)_{\theta \rightarrow \delta e}$ representations is due to $|\theta/\theta_c|$ not being unity at DC. The derived $(\gamma/\theta_c)_{\theta \rightarrow \delta e}$ transfer function is always below its approximation at DC by the same amount that θ/θ_c is below 0 db at DC. If $|\theta/\theta_c| = 1$ at DC, the approximation and derivation would lie practically on top of one another.

The SAS employed with BSL1 and AP1 differs from the above system, in that (i) the actuator lag τ_e is included; (ii) a parallel integrator has been inserted in the forward loop.* Without these two new features, the closed loop behavior of BSL1 and AP1 at low gain would be as in Figure 10, which shows the reduced bandwidth resulting from the gain change. The approximations are very good; $(\gamma/\theta_c)_{\theta \rightarrow \delta e}$ shows a big improvement over Figure 9 because $|\theta/\theta_c| \doteq 1$ at DC for BSL1 and AP1.

In Figure 11 the closed loop behavior of BSL1 and AP1 is shown with the parallel integrator and actuator lag now included. There is very little difference

* For the present, ignore the differing nature of the θ_c signals, although it may be noted that the SAS of Figure 7b, except for the presence of integral feedback, is conceptually similar to that of Figure 7a.

in $|\theta/\theta_c|$ for these aircraft whether these two components are included or not. Usually, a parallel integrator is inserted into the loop to improve the low frequency response. This was the case here as well, and some improvement in SAS performance was observed. The shape of θ/θ_c is practically unaffected by $\frac{s+a}{s}$ because ω_s' and $-a$ occur at about the same frequency. The zero partially cancels the second order factor in the denominator, making the net result akin to a first order pole near $-a$. This is about where $1/T_{sp1}'$ would be if $\frac{s+a}{s}$ were left out. Figure 12 depicts the system behavior at high gain. The bandwidth is increased so that the closed loop θ/θ_c behavior of BSL1 and AP1 at high gain is similar to that of the TG- configurations.

The actuator lag, being at such high frequency, naturally has little effect on the θ/θ_c closure. Its presence, however, creates the gain discrepancy between the approximate and derived transfer functions.

One may then draw the following conclusions:

- i) When $\theta \doteq \theta_c$, the approximate transfer functions are very precise for a large range of SAS gains, as long as actuator lags are neglected.
- ii) The parallel integrator in the forward loop has a small effect on gain and shape of θ/θ_c .
- iii) The inclusion of actuator lags makes the approximate transfer functions optimistic in gain; for more sophisticated SAS models, the derived transfer functions alone should be used in the analysis.

Because BSL1 and AP1 are products of a different research program than the other aircraft, they have more positive M_α , smaller M_q , $M_{\dot{\alpha}}$ and, as a rule, smaller Z_w than the other configurations. These differences have the greatest influence on the short period mode, which for all configurations is described by the two first order factors $1/T_{sp1}$ and $1/T_{sp2}$. Comparing Figure 10 to Figure 9, it is recognized that the more positive M_α of BSL1

and AP1 has shifted their short period roots to the right relative to the TG- configurations. The relatively low short period "damping" of BSL1 and AP1 also serves to place $1/T_{sp1}$ near the origin. This positioning of $1/T_{sp1}$ limits the SAS bandwidth to a lower value than that associated with the TG- aircraft, especially for low $1/T_{L\theta}$.

RESULTS AND DISCUSSION

Table V presents the experimental results in terms of pilot commentary and opinion rating. Because of the differences between the TG- and BSL1, AP1 aircraft, the former airplanes will be considered alone in Section I. BSL1 and AP1 will be introduced in later sections.

I. PILOT TECHNIQUE:

There is little difficulty in predicting the technique by which the pilot lands any of the TG- aircraft under consideration. One merely needs to know the position of the airplane in Figure 5b.

TG1A received the best pilot rating of the configurations studied. Its value of Z_w is large enough to compare favorably with the general aviation aircraft simulated in Reference 3. In the context of that report, its value of dy/dV identifies TG1A as a moderate floater.* Landing such an airplane is straightforward - the stick is used to execute the flare, assisted by a throttle reduction in the manner of the decelerate technique. Flight path control in the flare is very good, as evidenced by the nicely flat $(\gamma/\theta_c)_{\theta-\delta_e}$ response in Figure 9a. The vehicle is not enough of a floater to present any problems; it is easily landed with stick and throttle actions well correlated, in the manner preferred by the pilot.

When Z_w remains large, and dy/dV becomes more positive, the pilot gradually replaces the decelerate technique by the accelerate technique, consistent with the results of Reference 3. Figure 13a indicates, however, that increasing backsidedness tends to wash out the desired path correction. This suggests that with enough backsidedness, the throttle becomes the primary flare control, while the wheel is used to provide small corrections. In the case of TG1C, the pilot himself may not be certain whether the stick or throttle is more effective in the flare. With a large value of Z_w , the initial

*The variation in dy/dV of Reference 3 was

$$-1.25 \leq \frac{dy}{dV} \leq +.30 \text{ deg/kt}$$

stick response is quick enough to lead the pilot into trying a stick flare only to find that due to the backslidiness effect he is in for a hard touchdown. It is difficult for the pilot to find a consistent control technique which results in acceptable touchdowns, and he reflects his confusion in a poor rating for this aircraft.

Figure 13b shows that as Z_w is reduced in magnitude, the desired path correction due to stick action decreases. As $|Z_w|$ is reduced at constant $d\gamma/dV$, a value of Z_w is reached at which stick flares become marginal and the throttle must eventually be delegated as the primary controller.^{*} The airplane may no longer be adequately flared by an angle of attack change; the value of $1/T_{\theta_2}$, the high frequency $N_{\delta e}^{\theta}$ factor, becomes too low for the stick response to be snappy enough in the flare. Therefore TG4A and TG3C must be flared with the throttle. As power is added to TG4A to break the sink rate the airplane, which is already a moderate floater according to $d\gamma/dV$, now floats very badly. In order to land the aircraft, the pilot must paradoxically add some power to start the flare and later reduce power to set the aircraft down on the runway. These control reversals, with their associated timing difficulties, are quite annoying to the pilot. The problem is compounded in this case by the relatively small $(\gamma/\delta T)_{\theta-\delta e}$ bandwidth apparent in Figure 9b. To increase the pilot-vehicle system bandwidth, the pilot is required to provide more lead compensation in his control motions. A poor pilot opinion rating results. TG3C, with its low Z_w and positive $d\gamma/dV$, is immediately perceived by the pilot to be an aircraft for which throttle flares are essential. Control reversal is not necessary - a steady power addition is required. Nonetheless, the rating is poor, due perhaps to the difficulty of achieving consistent results in terms of the correct amount of power to be added. Once again, the $(\gamma/\delta T)_{\theta-\delta e}$ response, depicted in Figure 9d, is less than desirable.

While pilot technique may be accurately predicted for the airplanes with extreme values of $d\gamma/dV$ and Z_w , the procedure is not yet clear for aircraft lying between these TG- configurations. It is evident that more flight testing

^{*} The aircraft of Reference 3 all had sufficiently high Z_w to permit wheel flares.

is required to obtain this data. Nevertheless, several hypotheses are put forth in Figure 14 as to the location of the iso-opinion line in the $Z_x - \frac{dy}{dV}$ plane.

Figure 14a proposes a likely possibility. There is no doubt, in the light of the results of Reference 3 and the pilot ratings of the current experiment, that an optimum region exists in the neighborhood of TG1A. As one progresses vertically downward from the optimum, pilot opinion degrades as the decelerate technique becomes less effective. Moving vertically above the optimum, pilot rating worsens as the accelerate technique comes into play. Moving to the left, pilot ratings degrade slowly until a critical value of Z_x is reached, at which time the throttle becomes the primary control. The derivative Z_x is still large enough at this point for the stick to be used as a secondary control, making small corrections for throttle and gust inputs. The iso-opinion lines begin to bunch closely together when Z_x becomes low enough to make even small corrections impossible. The stick becomes merely a θ controller, adjusting the vehicle's attitude for level touchdown, while the flare must be made entirely with the throttle. When Z_x is low, backside airplanes are more amenable to a throttle flare than frontside ones, which exhibit aggravated floating tendencies requiring control reversals. Therefore the iso-opinion lines at low Z_x are biased in favor of positive dy/dV .

Because some areas of the $Z_x - \frac{dy}{dV}$ plane are suitable for throttle flares and some are suitable for stick flares, two optimum regions may exist as suggested in Figure 14b. Here, the best ratings are again near TG1A, but a second good region is indicated for the case where stick flares are impossible. A consequence of this format is that ratings necessarily worsen between the two optimums, reflecting, perhaps, the pilots' confusion when the two controls overlap in authority. As in the case of TG1C, the pilot may then be uncertain as to the correct procedure for successful touchdowns. Conversely, one might logically argue for an improvement in rating when two command inputs are available, since the pilot should be able to exert more precise control over the glide path.

A third possibility, Figure 14c, attempts to base throttle response on the throttle backsidedness parameter $(\Delta V_{ss} / \Delta \gamma_{ss})_{\Delta T}$ in the belief that it is a more relevant parameter to use for the throttle than dy/dV . Two sets of curves result, each valid in their domain.

It should be noted before closing this section that statements regarding pilot technique for the configurations tested are directly supportable from the data as typified in Figure 8.

II. EFFECT OF THROTTLE LAG:

In view of BSL1's position on the $Z_w - \frac{dy}{dV}$ plot, it comes as no surprise to find that the flare tends to be initiated with the throttle. The pilot rating for this aircraft at high gain, without turbulence and with $\tau_T = 0.4$ sec was almost as good as that of TG1A in spite of their wide separation in Figure 5b. This supports to some extent the contention that an optimum for throttle flares exists independently of one for stick flares. Both pilots were pleased with the attitude control available at this SAS gain, terming it "good" and "very comfortable - can put θ where I want it." For this aircraft, Z_w was still large enough to permit some stick compensation for small throttle errors during the flare.

The value of Z_w for AP1 is about half that of BSL1. For the case of AP1 at high gain, no turbulence and $\tau_T = 0.4$ sec, the throttle was again used to initiate the flare. However, the critical value of Z_w , beyond which the stick cannot be used to correct throttle input errors, has been exceeded for this configuration, as shown by the worsened pilot rating over BSL1. For AP1, the flare has to be entirely executed with the throttle, as the stick can be used solely to adjust θ for a level touchdown. As pilot 2 pointed out, the "low Z_w puts bigger demands on θ -control for last moment adjustments." The differing values of Z_w between TG3C and BSL1 at least partially explains the rating discrepancy there.

Pilot 2 alone flew BSL1 and AP1 with the two values of throttle lag. He noted these variations in pilot rating:*

	BSL1			AP1		
$\sigma_T =$	0	2.25	4.5	0	2.25	4.5
$\tau_T = 0.4$	3.5	4	6	4	5.5	7
$\tau_T = 1.5$	4.5	5	6.5-10	5.5	6.5	10

Although improvements of at least one rating point due to the shorter lag are observable in all instances, the most dramatic change is apparent at $\sigma_T = 4.5$ ft/sec.

With a 1.5 second throttle lag, the pilots have little choice but to use the throttle in an open loop manner. The critical choices in landing the aircraft involve the lead time and amount of power required in an open loop addition to produce a successful landing. The large leads associated with large τ_T are difficult to manage with precision. In a number of the landings a second, smaller throttle step, either positive or negative, was executed part way through the flare if a serious correction was required. In no case, however, can the pilots be said to be modulating the power in a closed loop manner. As pilot 1 says about BSL1 with no turbulence:

" $\dot{h} = \delta_T$ very sluggish; sometimes aircraft would appear to recover to acceptable \dot{h} and then drop in at very end, too late for recovery... best landings occurred when sink rate could be set up [on approach] and remained relatively undisturbed. This allowed smooth power addition and final θ adjustment to get good touchdown."

With increasing τ_T the pilots' closed loop control over throttle, and therefore over glide path, worsens steadily. Power must be added earlier in the flare, increasing the height of the flare initiation point and the flare time Δt .

* τ_T variations were flown in the case of high SAS gain only.

In the presence of turbulence the workload increases because of the variability of the flare initiation point, as dictated by the gust inputs to the aircraft. The effect of such random disturbances is magnified as τ_T increases since the pilot is exposed to them over a longer time period with little ability to correct for them, especially if Z_w is too low. Even at $\tau_T = 0.4$ sec, though, the pilot cannot be expected to monitor power in a completely closed loop fashion. Pilot 2 has suggested that a lag on the order of .25 seconds is required for that to be possible.

In further analysis of BSL1 and AP1, τ_T will be fixed at 1.5 sec.

III. EFFECT OF TURBULENCE:

As indicated above and confirmed in Table V, the presence of turbulence severely curtailed the pilot rating. For $\sigma_T = 2.25$ fps ($\frac{1}{2} T$), the pilot ratings degraded by $\frac{1}{2}$ - 1 point for the high gain SAS, and 1 - 1.5 points for the low gain SAS.* For the full turbulence level of $\sigma_T = 4.5$ fps (T), ratings were worsened a further 1.5 points for the low gain case and by the same for the high gain case, except for AP1 where the rating jumps from 6.5 to 10 between turbulence levels for pilot 2.

Turbulence was determined by the pilots not to affect the attitude control of the aircraft. This was a consequence of the properties of these configurations - M_α and M_u are both relatively small. Pilot 1, however, mentioned for BSL1 that "with turbulence, I like to use θ to provide some control over sudden changes near touchdown. This works out OK for high gain but is very marginal at low gain." Pilot 2 used this technique for no turbulence as well when flying BSL1.

Turbulence basically affected the timing of the landing maneuver and the selection of the flare initiation point. For each configuration tested, one may

* Although AP1 at low gain with turbulence was not flown, pilot 2 felt that it was probably a 9 at $\frac{1}{2} T$ and a 10 - "impossible" - at full turbulence. This goes along with the trend of AP1 being worse than BSL1 under any conditions, but it does suggest that a poor handling plane is affected to a greater extent by turbulence than a better one.

conceive of a "flare window" of acceptable values of h and γ at the flare initiation point. If the pilot is allowed to set up the aircraft on the approach so that it passes nicely through the flare window, he may consistently apply a certain control technique to land the airplane. Turbulence creates such a variability in the initial flare conditions that the pilot must think well ahead of the situation; power control was "difficult and critical due to the variability of the flare initiation point," in the words of pilot 2. Considerable touchdown dispersion results and for ratings in the 7-10 category, consistent landings were not achievable. Pilot 1 mentioned that, with full turbulence, "cannot stop last minute sinkers without either dropping in or overshooting with power and floating... need long runway to allow shallow flare." Turbulence is still a factor once the flare is begun, requiring the pilot to extend the flare and give himself time to apply glide path corrections.

IV. EFFECT OF SAS GAIN:

Pilot 1's ratings degraded $\frac{1}{2}$ point when the SAS gain was lowered, while pilot 2's opinion was a full point less. This is due to the increased pilot compensation, in the form of increased lead, which is required to extend the pilot-vehicle system bandwidth to an acceptable level.

		AP1	BSL1
δ_s lead	low gain	considerable	moderate
	high gain	moderate	minimal
δ_T lead	low gain	considerable	considerable
	high gain	considerable	moderate

The δ_T control has to be "early and right on" at low gain since, for BSL1, "can't fix things up with θ as well as high gain." For AP1, "it's impossible to fix things up with θ (low Z_w)." "

The high gain system of BSL1 and AP1 is not as tight as that used for the TG- airplanes, although from a handling qualities viewpoint there is not much difference, according to pilot 2, who flew both SAS's. It may be expected that increasing the tightness of the BSL1-AP1 SAS to that level would improve the pilot rating slightly. The θ response was usually termed "sluggish" for the low gain BSL1-AP1 SAS, "good" at his gain, and "snappy" for TG1A through TG3C.

LOAD FACTOR IN THE FLARE:

One of the conclusions drawn in Reference 3 is that there exists a good correlation between $\overline{\Delta n}$, the average load factor generated in the flare, and pilot opinion rating for the stick-only landings investigated there. The shape of this correlation is reproduced in Figure 15 for the 6° approach. Aircraft which tend to float require longer flares, at low $\overline{\Delta n}$, to bleed off enough speed before touchdown. Sinkers must be flared quickly, at high load factors, to prevent a hard landing. These extremes, being disliked by the pilot, receive relatively poor ratings. In the middle lies an acceptable region where the pilot can execute a straightforward maneuver, corresponding to $\overline{\Delta n} \doteq .08$ g.

Superimposed on this curve in Figure 15 are the average load factors generated in the flare for some of the configurations investigated in this report. The value shown for $\overline{\Delta n}$ is a simple average of the $\overline{\Delta n}$'s calculated for each individual landing. The differences between these values and the curve of Reference 3 are explored below.

TG1A, the easiest to land of the configurations investigated herein has a $\overline{\Delta n}$ corresponding to the optimum value of Reference 3. With its high Z_w and frontside dy/dV , it corresponds nicely to some of the aircraft examined there. Its pilot rating is better than those aircraft of Reference 3 because it is a two-control landing, with nicely correlated stick and throttle actions. As reference 3 indicates, any stick-only landing when $\frac{dy}{dV} < 0$ can be made more easily using the decelerate technique. The aircraft with low Z_w present a different

problem - the stick is no longer the primary controller. What kind of relation between $\overline{\Delta n}$ and pilot rating can one expect with these configurations?

A clue is provided in pilot 1's previous quotation about needing a long runway to allow a shallow flare when turbulence is present. As an aircraft with low Z_w becomes worse to handle, the danger of a very hard touchdown increases. The pilot reacts to this danger by applying more control lead and making a shallower, longer flare, giving him more time to correct for mistakes. With a conventional backside airplane this is not a feasible technique because of the danger of a high sink rate or stall as speed bleeds off. When a significant amount of lift is due to the powerplant, however, the lift loss due to deceleration in the flare can be recovered by adding power. Therefore, as the handling qualities of a STOL worsen, whether due to turbulence, SAS gain reduction or even configuration change, the average load factor generated in the flare may be expected to decrease because the flare time Δt is extended by the pilot.

This is not to say that the resulting landings are soft. After a long float the airplane could drop in hard at the end, producing \dot{h}_{TD} 's as large as 5 ft/sec. The larger \dot{h}_{TD} values give lower $\overline{\Delta n}$ because of the way the latter is calculated. The values of Z_w associated with the Reference 3 airplanes were sufficient to prevent such hard landings by generating enough $\overline{\Delta n}$ at the end of the flare to land softly. For most of the STOL aircraft discussed here, this capability was not present, so that the pilot rating versus $\overline{\Delta n}$ curve appears one-sided as in Figure 15. Nonetheless, there appears to be a good correlation between the two parameters for pilot ratings below 6.5 or so. The aircraft rated above this value are so hard to handle that no two landings are similar. The scatter in $\overline{\Delta n}$ due to this inconsistency produces unreliable results in the $\overline{\Delta n}$ calculation.

TG1C occupies a somewhat unusual position in Figure 15. If $\overline{\Delta n}$ were calculated for TG1C by the method of Reference 3, where \dot{h}_{TD} was assumed zero, it would occupy the primed position indicated, which is more or less proper in the context of that report.

For ratings less than 6.5 the effects of increased turbulence and of lower SAS gain are readily apparent in the decreasing $\overline{\Delta n}$. It is noted, however, that the correlation curve is steeper than that of Reference 3, suggesting that an increased standard of excellence is required by the pilot in the case of a two control landing. This is only natural because of the extreme difficulty involved in managing two controls properly. Closing loops on two independent controls is so difficult for the pilot that the rating he chooses is inevitably bad.

In spite of the correlation displayed in Figure 15, it may be logically argued that load factor is not a proper measure of STOL landing performance. The concept of relating $\overline{\Delta n}$ to pilot rating is based directly upon the amount of deceleration the aircraft experiences in the flare. In the case of STOL aircraft, speed behavior in the flare is usually ignored by the pilot. His main concerns are

- i) getting the aircraft into the touchdown zone, and
- ii) keeping \dot{h}_{TD} low, not necessarily in that order.

Military STOL transports currently under construction will achieve landings in the zone by means of a "no-flare" approach which generates \dot{h}_{TD} 's that are definitely unacceptable in the commercial passenger transport field. This "solution" neatly sidesteps the issue of what range of \dot{h}_{TD} is acceptable to passengers.

Rather than examine V- γ trajectories in the case of STOL aircraft, it may be more relevant to explore trajectories in the h- γ plane. Some are presented in Figure 16. An arbitrary range of acceptable γ_{TD} values corresponding to $\dot{h}_{TD} < 3$ fps has been selected. The increasing height of the flare initiation point with worsening handling qualities, corresponding to increasing Δt , is clearly indicated. A good landing is displayed in the case of BSL1 at high gain and no turbulence. The other two aircraft are typified by landings outside the acceptable zone. Just as $\overline{\Delta n}$ is related to flare trajectories in the V- γ plane, one could perhaps identify an analogous parameter with h- γ trajectories and

attempt to correlate pilot rating with it. On the other hand, one might carry the argument full circle and, deceleration in the flare aside, consider the effect of $\overline{\Delta n}$ on the $h-\gamma$ trajectories. Increasing $\overline{\Delta n}$ tends to rotate the trajectories of Figure 16 clockwise with respect to the coordinate axes. Up until the last few feet above the runway, the trajectories of Figure 16 remain similar. It is only the difficulty experienced in generating enough load factor in the last moments before touchdown which separates good airplanes from unacceptable ones. Perhaps a load factor calculation weighted more heavily toward the last part of the flare maneuver may be of significance.

VI. EFFECT OF $Z_{\delta T}$ INCREASE:

A very few landings were executed in BSL1 with its normal values of $X_{\delta T}$ and $Z_{\delta T}$ doubled. This adjustment slightly improved throttle control in the flare. Pilot 2 indicated that the improvement in terms of pilot rating was indeed small - on the order of $\frac{1}{2}$ point. Pilot 1 asserted that the $Z_{\delta T}$ increase "did not help. It may have been worse due to larger effect and sluggish response (response to wrong input is too high)."

VII. RATE COMMAND VS ATTITUDE COMMAND:

Pilot 2 has made a good many landings with both the TG- and BSL1, AP1 configurations. His preference is for the rate command system, especially during the approach since airplane control force trim is automatic when rate command is used. For the aircraft studied here, there is little difference between systems in the flare because the relatively sluggish pitch dynamics associated with STOL transports makes the stick action about the same for both types of SAS's. The tendency, when first confronted with a rate command system, is to overflare the airplane. A pilot must become accustomed to releasing the stick slightly. A few trials, however, can easily familiarize the typical pilot with the rate command system. For these reasons it is felt that, in this experiment, the pilot ratings discussed above are independent of the form of command input.

SUGGESTIONS FOR FURTHER RESEARCH

1. When the primary control used in performing the flare maneuver is easily identified, a prediction of pilot technique is straightforward. Unfortunately, little is known to date concerning the pilot's control of the airplane for values of Z_w and $d\gamma/dV$ where throttle and stick compete more or less equally for authority. Furthermore, it may prove to be inappropriate to associate $d\gamma/dV$ with pilot rating for low Z_w aircraft. The $(\Delta V_{ss}/\Delta \gamma_{ss})_{\Delta T}$ parameter may logically have more meaning where throttle flares are concerned, leading to the two sets of iso-opinion contours of Figure 14c. More flight testing is required to establish the iso-opinion contours for variations in Z_w , $d\gamma/dV$, and $(\Delta V_{ss}/\Delta \gamma_{ss})_{\Delta T}$.

2. Deceleration in the flare does not appear to be a factor in the landing of STOL airplanes. Reference 7 even suggests that speed control in the approach is of little concern to the pilot! This statement underscores a major difference in the handling of these two types of aircraft which remains to be fully explored. It is unclear at this time what the "proper" approach speed for a STOL might be, or even if one exists. What factors govern the selection of approach speed for STOL airplanes? The upper limit is governed by the short landing distance demanded of STOL aircraft. On the other hand, a lower limit must exist, or else one could land at zero speed all the time. From an aerodynamic point of view, wing stall is not a limiting factor; because a good deal of the aircraft's weight is supported by vectored thrust, the lift coefficient of the wing in the approach configuration is not, in most cases, close to $C_{L_{max}}$. There is a limit, however, on how slow one may go, since the aircraft is not one hundred percent supportable by vectored thrust alone. This consideration must be one of several on which a selection of approach speed is based.

3. Consistency, in terms of touchdown point and \dot{h}_{TD} , is the real measure of success in the landing of any aircraft. It is unfortunate that, in the near future, a powered-lift STOL is not likely to be built which a pilot can land in the zone at zero sink rate practically every time. The random variations introduced by turbulent gusts or other factors seem to make each landing a unique experience. Sophisticated electronic aids such as flight directors, for example, have been introduced to reduce the scatter in the results but it appears that in order to restrict the variability of the touchdown point one will have to accept nonzero sink rates at touchdown. What constitutes an acceptable \dot{h}_{TD} is a matter for conjecture. If reducing touchdown dispersion is the overriding concern, then it may be best not to flare the aircraft at all, but rather make it structurally sound enough to withstand flying straight on to the runway without harm. This, the military solution, is a hard one to accept in the case of passenger aircraft. With the latter, some compromise between touchdown distance and \dot{h}_{TD} will most likely be effected, though the actual mix of acceptable values of both variables has yet to be determined.

4. Both pilots in this program asserted that they did not concern themselves with closed loop speed control in the flare. Even in the case of conventional aircraft, speed control in the flare is not attempted, assuming that a proper approach speed is maintained up to the flare initiation point. Deceleration of conventional aircraft in the flare is important as the cause of the large sink rates perceived by the pilot in the cases where speed loss is extensive. However, it is the pilot's sensory perception of h and \dot{h} which influences his control actions. In this regard, flare trajectories in the h - γ plane may be more meaningful than those in the V - γ plane.

The shape of the trajectories in both planes is related to the load factor generated in the flare. Although a value of $\overline{\Delta n}$ is not uniquely related to a particular flare, the pilot's control action in executing an ideal landing in a particular

aircraft generates a value of $\overline{\Delta n}$ which he tries to attain in every touchdown maneuver. There is, then, a correlation between success in the flare, as reflected in pilot rating, and $\overline{\Delta n}$. The shape of this correlation is not necessarily invariant among aircraft types, as indicated in Figure 15.

CONCLUSIONS

The following conclusions apply to landings executed in STOL transport aircraft with powered-lift capability. They are based on the experimental results presented above. Because more experimentation will be required to explore the STOL landing in sufficient detail, these conclusions may be considered tentative.

1. At the flare initiation point, the pilot is most concerned with altitude and sink rate. Acceptable values of these variables comprise the "flare window." Future research will have to determine the effect, if any, of airspeed at this point. If the pilot can hit the flare window consistently, he may be expected to identify a control technique which will enable him to flare the aircraft with confidence.

2. For aircraft with relatively tight SAS's and short actuator lags, knowledge of Z_w and dy/dV should enable one to predict the flare technique in calm air. For such aircraft, pilot opinion contours in the $Z_w - \frac{dy}{dV}$ plane appear able to provide a prediction of pilot rating for the flare, once the proper set of contours is established.

3. Low SAS gain, large throttle lag, or turbulence influences the maneuver by impairing the pilot's ability to hit the flare window. The pilot reacted in this experiment by increasing the height of the flare initiation point, giving himself more time and altitude in which to correct high sink rates.

4. Load factor in the flare is correlated with pilot rating in this experiment. The shape of the correlation appears to differ from that for conventional aircraft. Turbulence, as well as changes in SAS gain, was felt to influence $\overline{\Delta n}$.

5. The pilot commentary leads one to conclude that speed was not controlled by the pilots during the flare. It appears that excessive deceleration was not a factor because of the powered-lift capability of the aircraft.

REFERENCES

1. Franklin, J. A. and Innis, R. C., "Flight-Path and Airspeed Control for the STOL Approach and Landing," STOL Technology, NASA SP-320, Oct. 1972, pp. 181-198.
2. Craig, S. J. and Heffley, R. K., "Factors Governing Control in a STOL Landing Approach," Journal of Aircraft, Vol. 10, No. 8, Aug. 1973, pp. 495-502.
3. Seckel, E. and Whyte, P. H., "Flight Mechanics and Pilot Evaluation of Conventional Landings," SAE Paper 750529, Apr. 1975.
4. Ellis, D. R., "General Aviation Landing Research at Princeton University," SAE Paper 730306, Apr. 1973.
5. Galloway, R. T., Jr., "In-Flight Simulation of the Longitudinal Characteristics of a Powered Lift STOL Aircraft," Princeton University Report No. 1124-T, Nov. 1973.
6. Franklin, J. A. and Innis, R. C., Flight-Path and Airspeed Control During Landing Approach for Powered-Lift Aircraft, NASA TN D-7791, Oct. 1974.
7. Craig, S. J., Hoh, R. H., and Jewell, W. F., "Identification of Minimum Acceptable Characteristics for Manual STOL Flight Path Control," STI TR 1035-3R, Vol. I, June 1976, Vol. II, July 1975.
8. Regev, Z., "Effects of Variations in Approach Conditions and 'Ground Effect' on the Ease and Quality of Landing," Princeton University Report No. 1134-T, Nov. 1973.

TABLES

Variations in turbulence level and SAS gain with respect to BSL1 and AP1 will be indicated by the notation

BSL1, j ℓ AP1, j ℓ

where $j = \begin{cases} \text{H} & \text{high gain SAS} \\ \text{L} & \text{low gain sas} \end{cases}$

$\ell = \begin{cases} 0 & \text{no turbulence} \\ \frac{1}{2} & \sigma_T = 2.25 \text{ ft/sec} \\ \text{T} & \sigma_T = 4.5 \text{ ft/sec} \end{cases}$

The two pilots will be identified by:

P1 = pilot 1

P2 = pilot 2

TABLE I: OPEN LOOP TRANSFER FUNCTIONS

	Δ_L $(\frac{1}{T_{sp1}})(\frac{1}{T_{sp2}})[\zeta_p; \omega_p]$ $(\frac{1}{T_{p1}})(\frac{1}{T_{p2}})$	$N_{\delta e}^{\theta}$ $[\theta; \omega_{\theta}]$ $(\frac{1}{T_{\theta1}})(\frac{1}{T_{\theta2}})$	$N_{\delta e}^{\gamma}$ $(\frac{1}{T_{\gamma1}})$	$N_{\delta T}^{\gamma}$ $(\frac{1}{T_{\gamma T1}})(\frac{1}{T_{\gamma T2}})(\frac{1}{T_{\gamma T3}})$
BSL1	(-.143)(1.123)[.434;.308]	[.909;.290]	(-.053)	(.155)(-.217)(1.119)
AP1	(.049)(.828)[.311;.278]	[.517;.318]	(.011)	(.031)(.279)(.541)
TG1A	(.801)(1.838)[.860;.096]	(.169)(1.285)	(.132)	(.162)(.281)(1.069)
TG2A	(.600)(1.246)[.745;.101]	(.177)(.470)	(.115)	(.160)(.281)(1.069)
TG3A	(.519)(1.199)[.767;.096]	(.189)(.318)	(.113)	(.161)(.281)(1.069)
TG4A	(.478)(1.144)[.864;.084]	[.988;.210]	(.117)	(.159)(.281)(1.069)
TG1C	(.690)(1.910)[.266;.254]	(.179)(1.206)	(-.052)	(.072)(.281)(1.069)
TG3C	(.444)(1.164)[.161;.184]	[.792;.200]	(-.075)	(.068)(.281)(1.069)
G1/ U1	(.611)(1.236)(.044)(.115)	(.172)(.485)	(.141)	(.181)(.281)(1.069)
G1/ U0	(.597)(1.247)[.942;.102]	(.220)(.466)	(.154)	(.212)(.281)(1.069)
G1/ U2	(.597)(1.248)[.693;.108]	(.179)(.466)	(.109)	(.127)(.281)(1.069)
G1/ U4	(.614)(1.234)(.029)(.131)	(.169)(.489)	(.146)	(.133)(.281)(1.069)
G1/ U8	(.617)(1.231)(.081)(.145)	(.168)(.493)	(.153)	(.123)(.281)(1.069)
G3/ U2	(.513)(1.350)[- .021;.310]	[.869;.287]	(-.279)	(.074)(.281)(1.069)
G3/ U4	(.538)(1.310)[.146;.237]	[.986;.287]	(-.099)	(.050)(.281)(1.069)
G3/ U8	(.562)(1.282)[.307;.183]	(.209)(.397)	(.005)	(.032)(.281)(1.069)
G5/ U4	(.525)(1.333)[- .014;.283]	[.948;.264]	(-.234)	(.040)(.281)(1.069)
G5/ U8	(.539)(1.308)[.155;.234]	[.989;.288]	(-.092)	(.026)(.281)(1.069)

TABLE II: STABILITY DERIVATIVES

Derivative	BSL1	AP1	TG1A	TG4A	TG1C	TG3C
X_u	-.101	-.069	-.154	-.147	-.085	-.077
Z_u / V_o	-.00332	-.00306	-.0014	-.0004	-.0088	-.0018
M_u	.000262	-.000145	0	0	0	0
X_a	12.42	27.25	12	12	12	12
Z_a / V_o	-.427	-.260	-1.30	-.27	-1.30	-.24
M_a	.177	-.044	-.300	-.300	-.300	-.300
$M_{\dot{a}}$	-.112	-.112	-.420	-.420	-.420	-.420
$X_{\delta T}$.0264	.0147	.0064	.0322	-.0016	-.0052
$Z_{\delta T} / V_o$	-.000373	-.000745	-.00107	-.00107	-.00107	-.00107
$M_{\delta T}$	-.000147	.000111	0	0	0	0
M_q	-.6091	-.6091	-.930	-.930	-.930	-.930
$M_{\delta e}$	-.702	-.700	-1.20	-1.20	-1.20	-1.20

TABLE III

III-A: CLOSED LOOP TRANSFER FUNCTIONS; NO τ_e , $\frac{s+a}{s}$:
$$\frac{\theta}{\theta_c} = \frac{N_{\delta_c}^{\theta}}{\Delta_L'} \quad \left(\frac{\gamma}{\theta_c}\right)_{\theta-\delta_e} = \frac{N_{\delta_e}^{\gamma}}{\Delta_L'} \quad \left(\frac{\gamma}{\delta_T}\right)_{\theta-\delta_e} = \frac{N_{\delta_T}^{\gamma'}}{\Delta_L'}$$

	Δ_L'			$N_{\delta_T}^{\gamma'}$			
	$\left(\frac{1}{T_{sp1}}\right)$	$\left(\frac{1}{T_{sp2}}\right)$	$[\zeta_p'; \omega_p']$	$\left(\frac{1}{T_{\gamma T_1}}\right)$	$\left(\frac{1}{T_{\gamma T_2}}\right)$	$\left(\frac{1}{T_{\gamma T_3}}\right)$	
BSL1, L	(.115)	(1.942)	[.665; .444]	(.155)	(.221)	(2.081)	low gain SAS
AP1, L	(.366)	(1.771)	[.464; .338]	(.031)	(.485)	(1.785)	
TG1A	(.174)	(3.128)	[.960; .991]	(.162)	(.972)	(2.778)	
TG4A	(.946)	(2.834)	[.957; .202]	(.159)	(.972)	(2.778)	
TG1C	(.214)	(3.190)	[.921; .940]	(.072)	(.972)	(2.778)	
TG3C	(.935)	(2.838)	[.711; .207]	(.068)	(.972)	(2.778)	

III-B: CLOSED LOOP TRANSFER FUNCTIONS; τ_e , $\frac{s+a}{s}$ INCLUDED:
$$\frac{\theta}{\theta_c} = \frac{\frac{1}{\tau_e} (s+a) N_{\delta_e}^{\theta}}{\Delta_L'} \quad \left(\frac{\gamma}{\theta_c}\right)_{\theta-\delta_e} = \frac{N_{\delta_e}^{\gamma}}{\Delta_L'} \quad \left(\frac{\gamma}{\delta_T}\right)_{\theta-\delta_e} = \frac{N_{\delta_T}^{\gamma'}}{\Delta_L'}$$

	Δ_L'				$N_{\delta_T}^{\gamma'}$		
	$\left(\frac{1}{T_{sp1}}\right)$	$\left(\frac{1}{T_{sp2}}\right)$	$[\zeta_{SAS}'; \omega_{SAS}']$	$[\zeta_p'; \omega_p']$	$\left(\frac{1}{T_{\gamma T_1}}\right)$	$\left(\frac{1}{T_{\gamma T_2}}\right)$	$\left(\frac{1}{T_{\gamma T_3}}\right)$
BSL1, L	(2.114)	(8.292)	[.735; .162]	[.597; .504]	(.155)	(.221)	(2.081)
AP1, L	(1.905)	(8.305)	[.9 .740]	[.490; .362]	(.031)	(.485)	(1.785)
BSL1, H	(1.716)	(7.911)	[.841; .192]	[.842; .769]	(.155)	(.609)	(2.485)
AP1, H	(.215)	(7.929)	[.545; .331]	[.930; 1.367]	(.031)	(.876)	(2.186)

TABLE IV: LANDING DATA

Configuration	Touchdown distance (ft) if available	Flare time Δt (sec)	Load factor $\overline{\Delta n}$ (g)	Deceleration ΔV (kt)
TG1A	600	6.0	.066	5.7
	350	7.3	.060	6.7
	50	4.4	.077	5.0
		4.1	.079	3.1
		4.2	.076	4.3
		6.4	.058	6.2
		4.5	.079	5.5
		4.8	.063	4.3
TG4A	+600	7.7	.046	3.0
	170	6.4	.046	3.2
		3.9	.082	3.0
		3.4	.049	2.9
		4.6	.060	2.6
	110	4.3	.063	3.6
TG1C	55	6.9	.072	5.4
	60	5.2	.087	5.2
		3.8	.086	3.7
	160	5.0	.081	6.5
	200	5.2	.066	5.8
	20	3.6	.086	3.9
	80	3.9	.094	4.5
TG3C	220	11.7	.038	7.0
	70	5.3	.049	6.9
		4.4	.085	3.6

TABLE IV (continued)

Configuration	Touchdown distance (ft) if available	Flare time Δt (sec)	Load factor $\overline{\Delta n}$ (g)	Deceleration ΔV (kt)
BSL1, HO	200	4.5	.057	4.7
	-100	4.2	.055	4.3
	50	4.2	.067	2.8
	100	9.1	.058	6.3
	300	7.6	.075	6.5
	300	6.9	.072	3.5
	150	9.2	.049	4.8
	250	6.7	.051	3.9
	- 50	5.1	.055	1.2
	100	4.0	.082	2.8
BSL1, H $\frac{1}{2}$	100	9.2	.068	5.4
	250	6.7	.053	2.8
	250	4.8	.050	4.5
	200	5.3	.066	4.0
BSL1, HT	250	7.2	.060	5.5
	250	8.0	.061	6.0
	-100	3.1	.085	2.0
	+100	4.9	.096	2.9
	75	3.4	.085	4.1
	0	3.1	.070	4.8
	300	12.2	.057	7.0
	350	5.0	.058	1.5
BSL1, LO	- 20	9.1	.044	4.5
	- 10	3.9	.060	4.6
	0	13.3	.044	3.0
	150	8.3	.064	5.7
	0	7.1	.050	4.6
	100	8.2	.055	5.1
	400	9.2	.056	3.1

TABLE IV (continued)

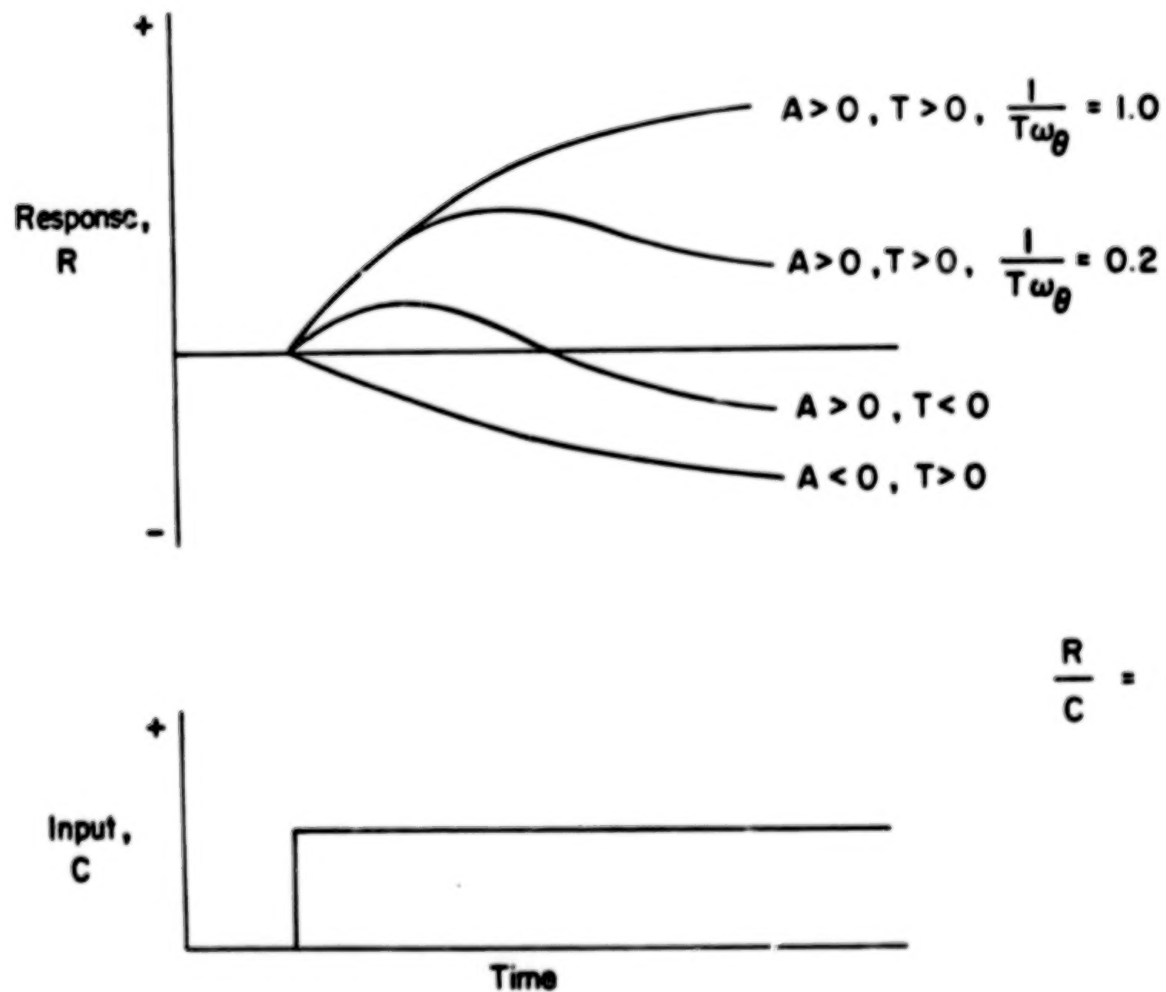
Configuration	Touchdown distance (ft) if available	Flare time Δt (sec)	Load factor $\overline{\Delta n}$ (g)	Deceleration ΔV (kt)
BSL1, L $\frac{1}{2}$	150	8.7	.051	3.1
	450	12.3	.054	7.2
BSL1, LT	300	4.3	.040	2.3
	250	9.3	.057	6.2
AP1, HO	225	6.5	.049	4.6
	75	5.0	.073	5.6
	100	3.9	.054	2.9
	150	5.1	.037	5.9
	225	10.6	.037	6.5
	- 20	6.9	.054	5.1
	+600	9.2	.044	5.5
	- 50	8.7	.044	6.5
	+150	8.8	.056	6.2
	100	6.1	.051	4.5
	175	4.9	.073	5.1
	175	8.1	.061	3.2
AP1, H $\frac{1}{2}$	300	11.2	.033	6.0
	250	7.7	.051	5.2
AP1, LO	200	7.9	.050	5.6
	500	8.2	.052	9.5
	- 50	8.6	.050	4.3
	225	5.3	.069	5.3
	- 50	12.6	.035	5.5
	175	4.3	.053	3.0

TABLE V: PILOT RATINGS AND COMMENTARY

Configuration	Pilot Rating	Commentary
TG1A	3.0	-easy to flare.
TG4A	5.5-7.0	-troubles with overflaring; tend to balloon. -power addition needed, but hard to get right combination; δ_T reversal in flare.
TG1C	6.0-7.0	-don't need power unless speed is low. -sinks in flare; firm touchdowns.
TG3C	6.0-7.0	-power flare; apprehensive about low Z_w .
BSL1, HO	P1 = 4.5 P2 = 4.0	-open loop power at ~50 ft; start θ change to touchdown attitude at 35-40 ft; control final sink with attitude. -can get desired performance with practice; main problem is to bring in power at right time.
BSL1, $H_{\frac{1}{2}}$	P1 = 5.0 P2 = 5.0	-considerable lead required in \dot{h} control. -worsened rating over HO because of increased $\dot{h} - \delta_T$, $\dot{h} - \theta$ compensation against gusts.
BSL1, HT	P1 = 7.0 P2 = 6.5-10	-definitely cannot attain adequate performance. -need long runway to allow shallow flare; even then workload is extreme to get reasonable touchdown.
BSL1, LO	P1 = 5.0 P2 = 5.0	-same as with high gain except poor control of θ makes airplane unforgiving of errors just before touchdown.
BSL1, $L_{\frac{1}{2}}$	P1 = 6.5 P2 = 6.0	-need good control of θ right near touchdown to regulate against last minute gusts; this is not at all precise with low gain SAS. - \dot{h} control difficult and critical due to variability of flare initiation point; working hard, thinking ahead of situation.

TABLE V (continued)

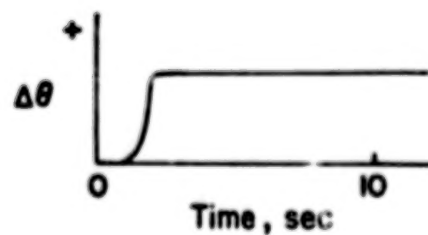
Configuration	Pilot Rating	Commentary
BSL1, LT	P1 = 8.0 P2 = 7.0-10	-on runs with significant gusts, one can't count on successful landing. -cannot stop last minute sinkers without either dropping in or overshooting with power and float-ing. -good landing seems too dependent on luck.
AP1, HO	P1 = 6.5 P2 = 5.5	-considerable compensation for thrust lag and slower than desirable attitude control. -low Z_w puts bigger demand on θ -control for last moment adjustments.
AP1, H $\frac{1}{2}$	P2 = 6.5	-working <u>very</u> hard to get acceptable performance.
AP1, HT	P2 = 10	-can't cope.
AP1, LO	P1 = 7.0 P2 = 6.5	-considerable throttle compensation - have to be early and right on since it's impossible to fix up with θ (low Z_w).



$$\frac{R}{C} = \frac{A(s + 1/T)}{s^2 + 2\zeta_0 \omega_0 s + \omega_0^2}$$

FIGURE 1. TIME RESPONSE CHARACTERISTICS

(a.) ATTITUDE CHANGE
CONSTANT THRUST



(b.) THRUST CHANGE
CONSTANT ATTITUDE

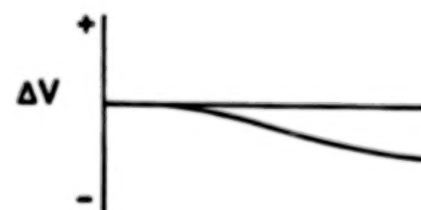
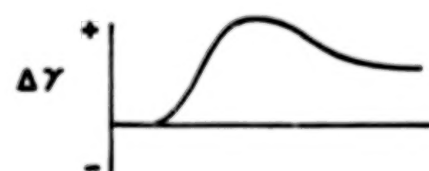
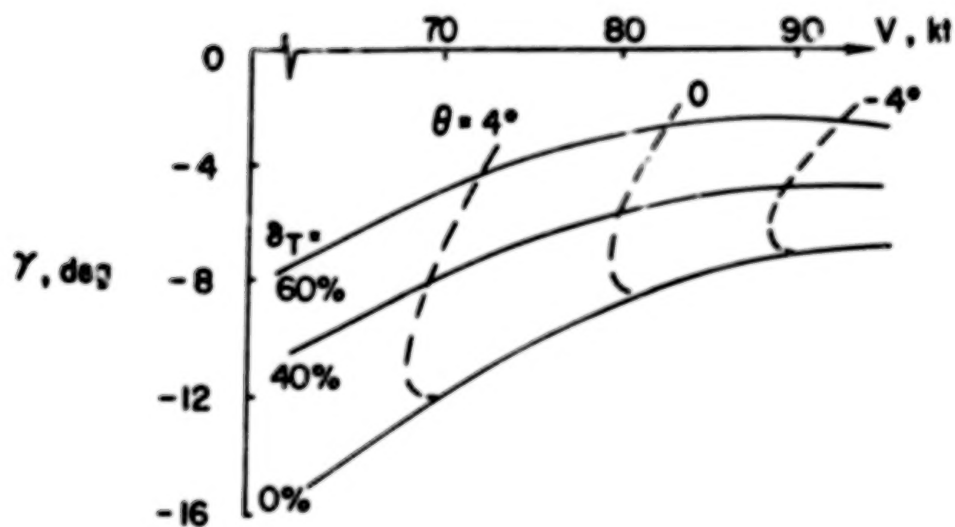
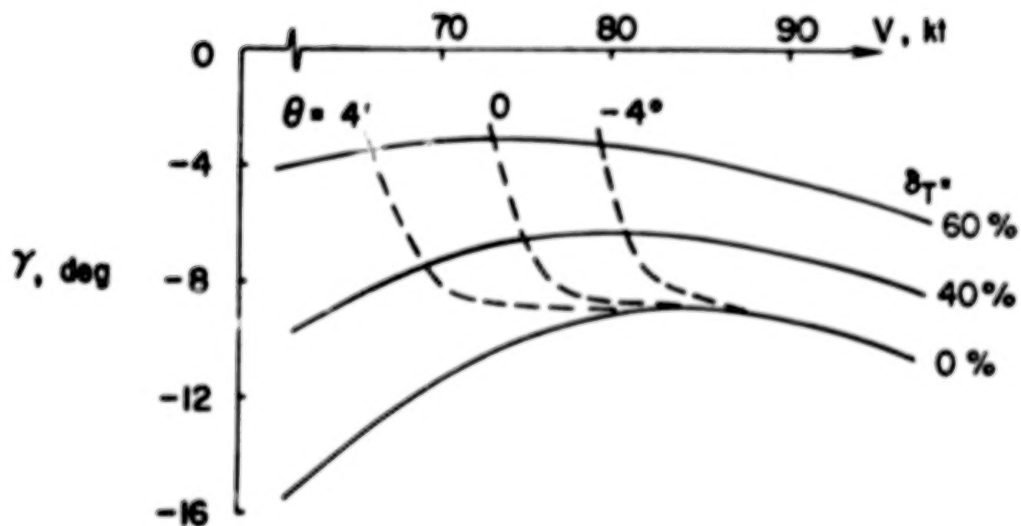


FIGURE 2. FLIGHT PATH AND AIRSPEED RESPONSE



(a.) BSLI - PROVERSE COUPLING



(b.) API - ADVERSE COUPLING

FIGURE 3. STEADY STATE PROPERTIES

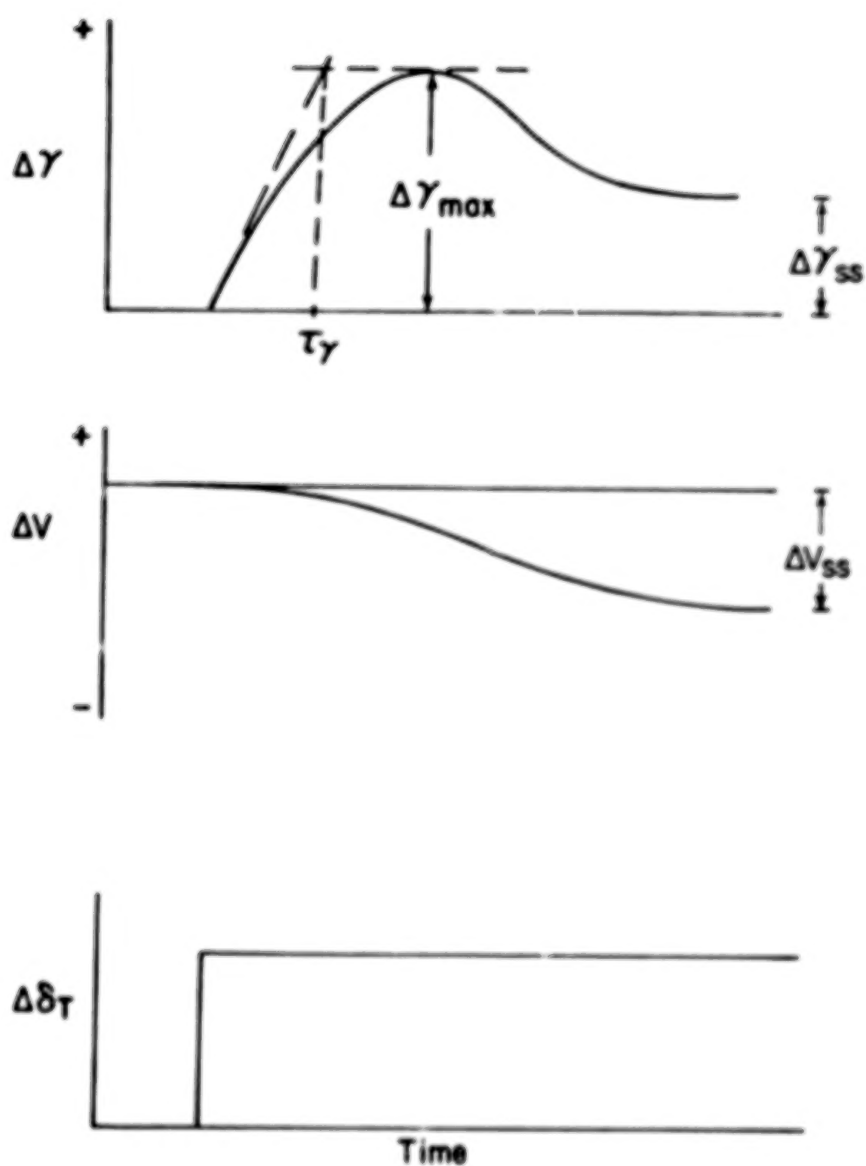


FIGURE 4. DEFINITION OF THROTTLE RESPONSE PARAMETERS

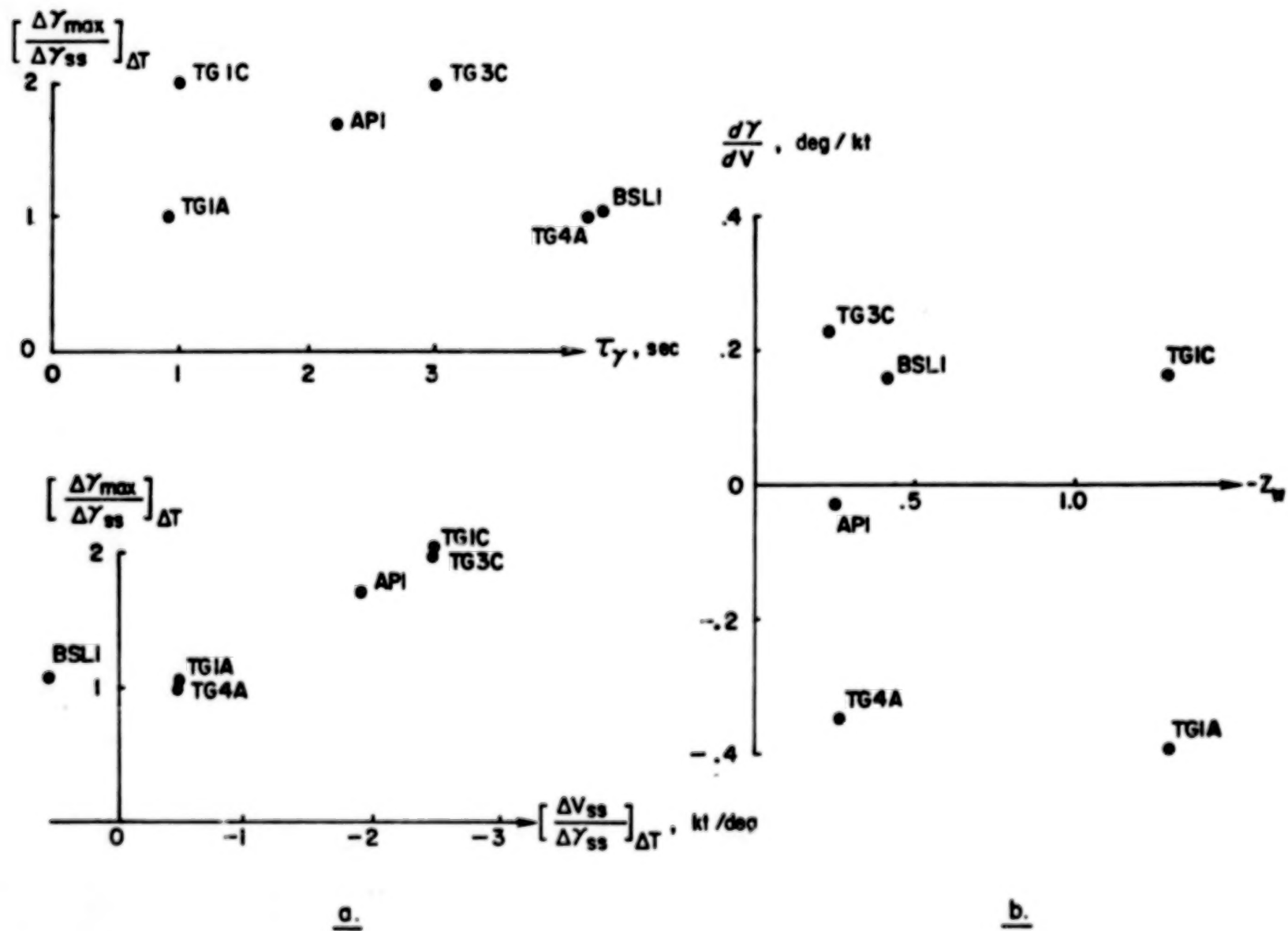
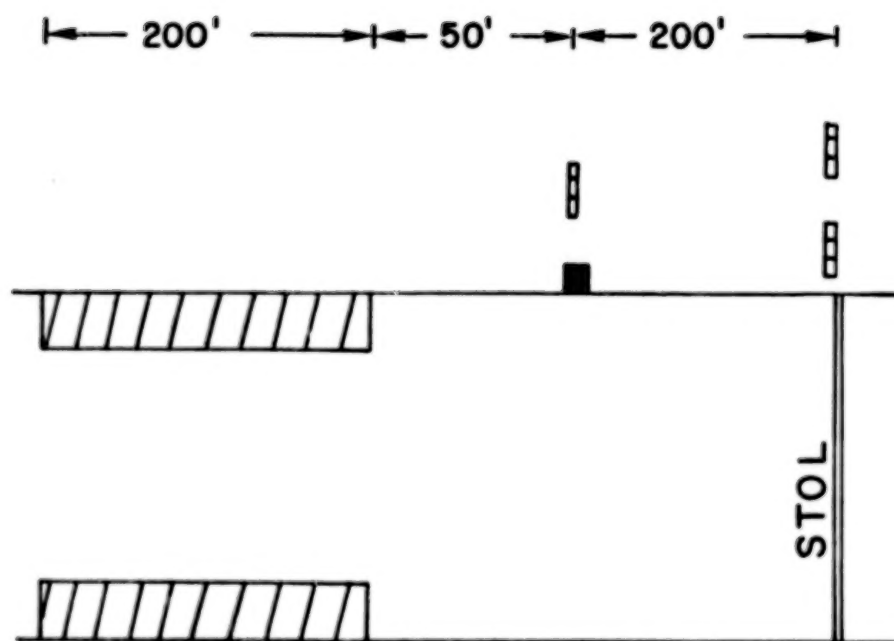
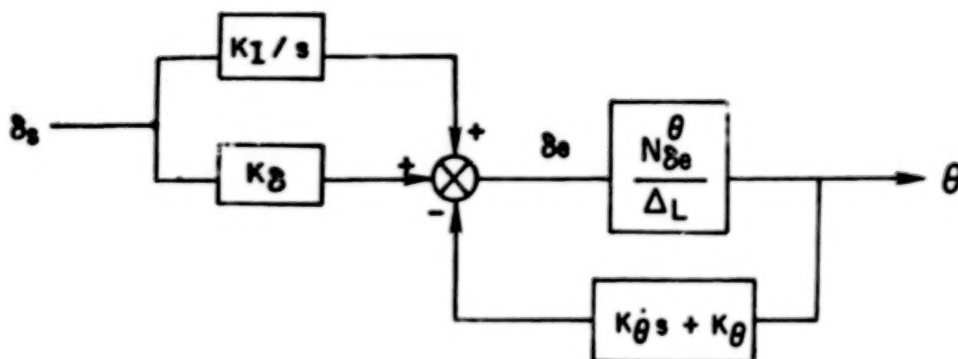


FIGURE 5. RESPONSE CHARACTERISTICS OF SELECTED CONFIGURATIONS



- TALAR
- ⌐ Glide Slope Lights
- ▨ Boundaries of STOL Zone

FIGURE 6. STOL RUNWAY SETUP



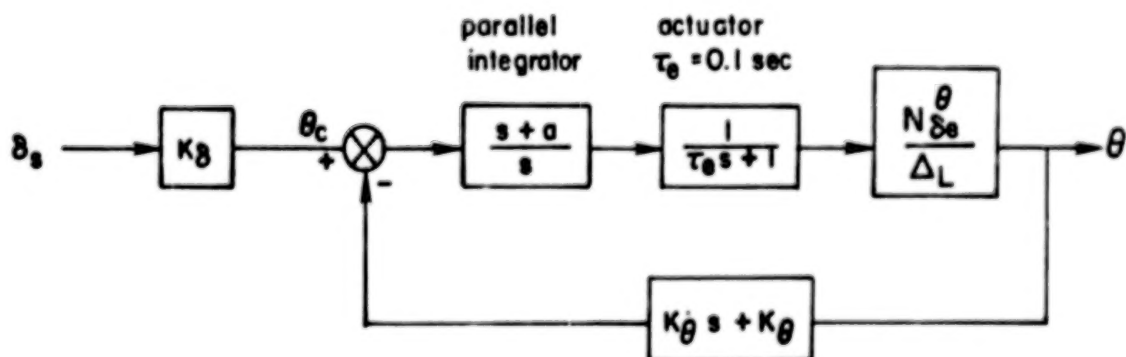
$$K_I = 1.5$$

$$K_\theta = 2.0$$

$$K_B = 1.5$$

$$K_{\dot{\theta}} = 2.0$$

FIGURE 7a. RATE COMMAND/ATTITUDE HOLD SAS



	K_θ	$K_{\dot{\theta}}$	K_{θ_c}	a
Low Gain	1.0	2.0	4.0	0.2
High Gain	2.5	2.5	10.0	0.0

FIGURE 7b. ATTITUDE COMMAND/ATTITUDE HOLD SAS

TG3C

TG1A

TG4A

TG1C

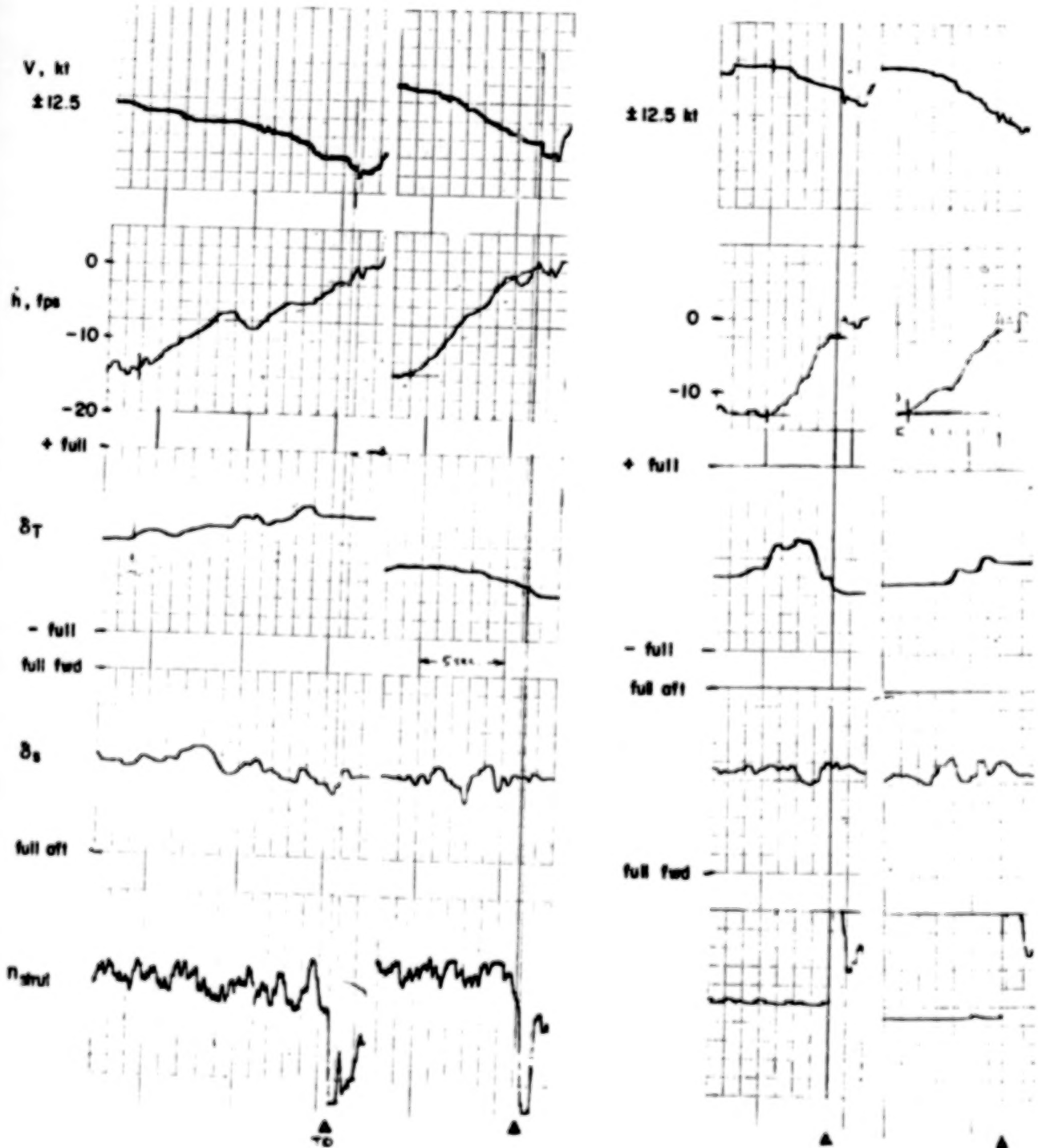


FIGURE 8a. ACTUAL LANDINGS WITH THE TG- AIRCRAFT

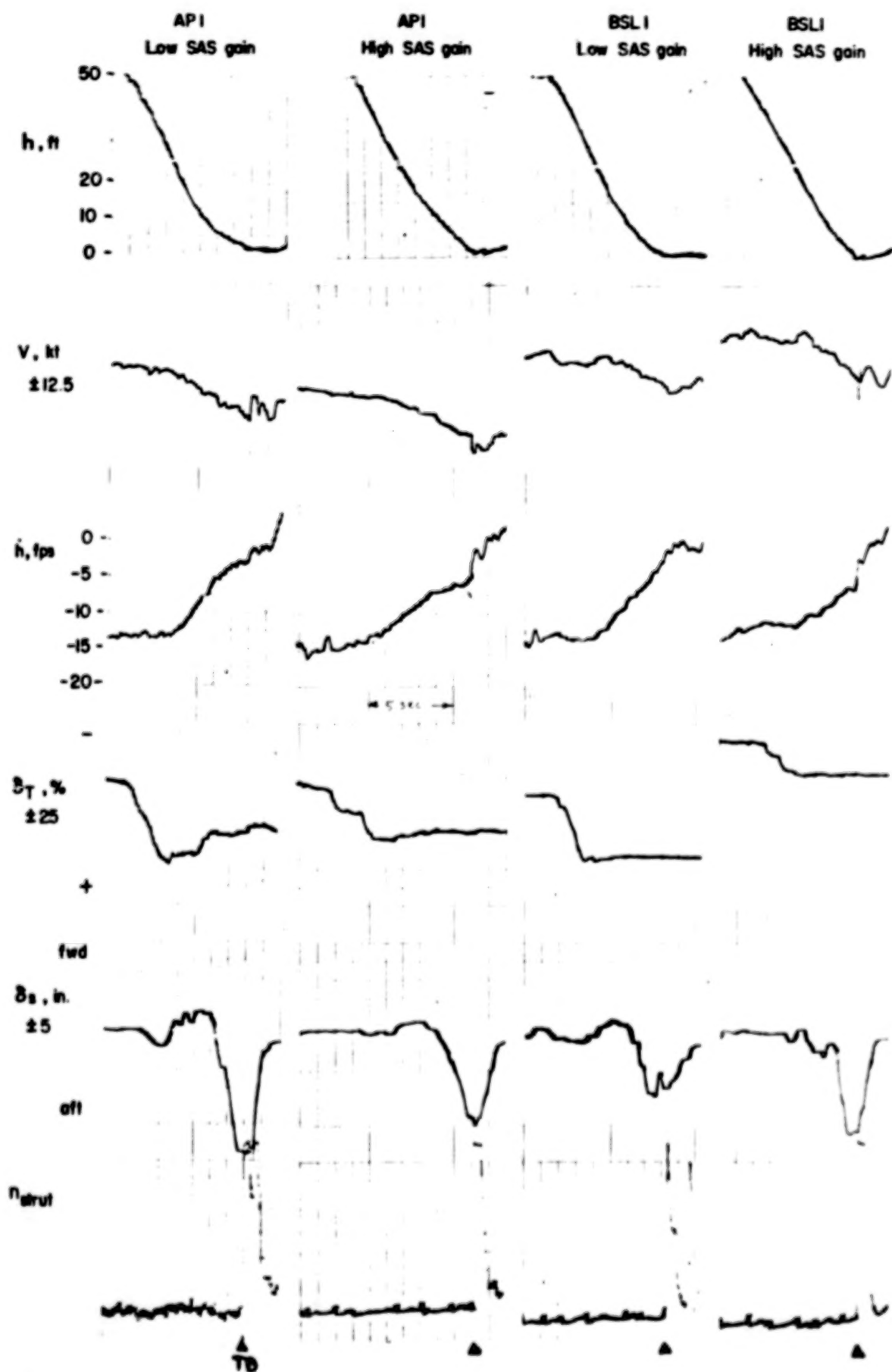


FIGURE 8b. ACTUAL DATA LANDINGS WITH BSLI AND API, $\tau_T = 1.5$ sec., $\sigma_u = 0$.

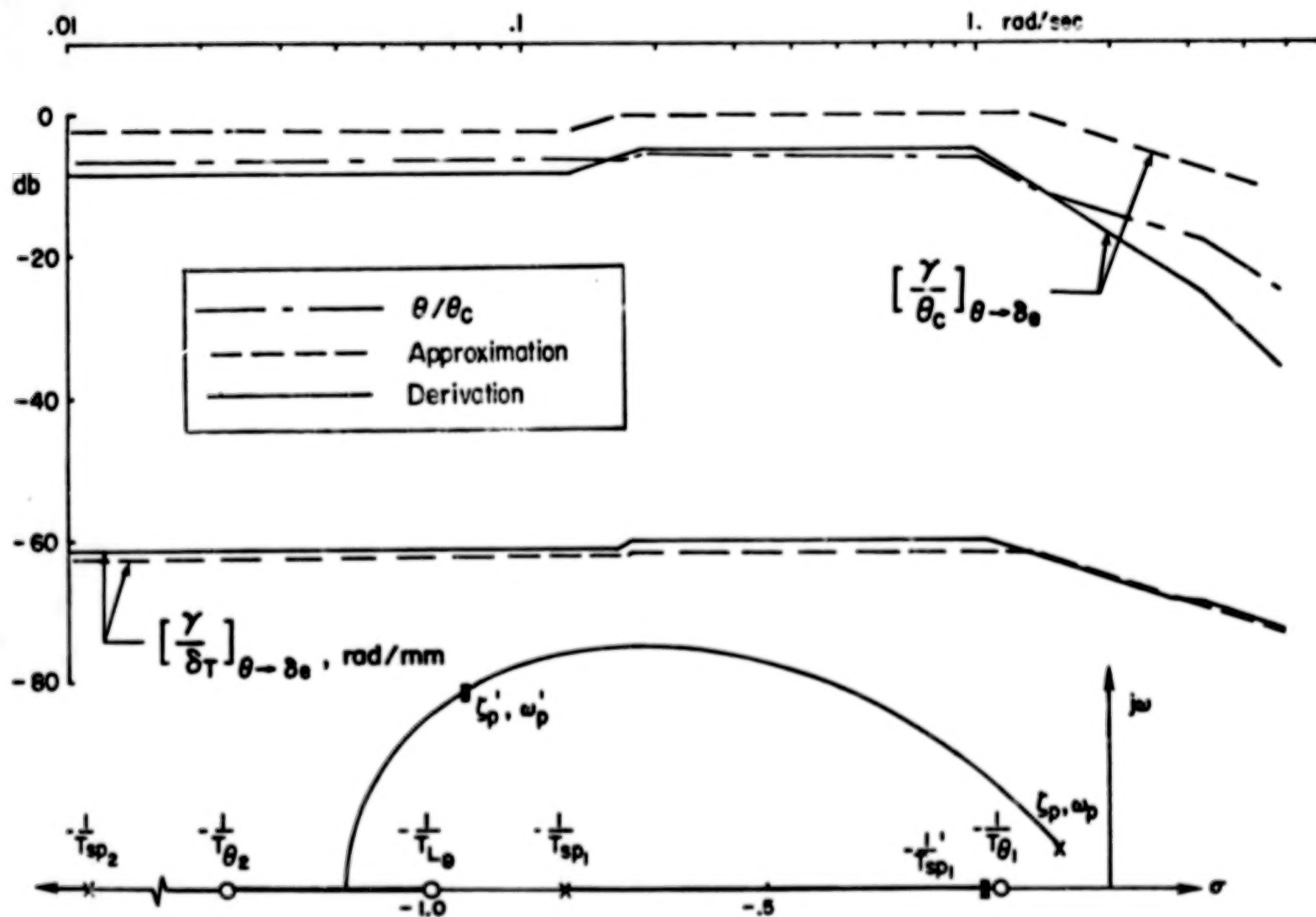


FIGURE 9a. TGLA: CLOSED LOOP FREQUENCY RESPONSE AND ROOT LOCUS

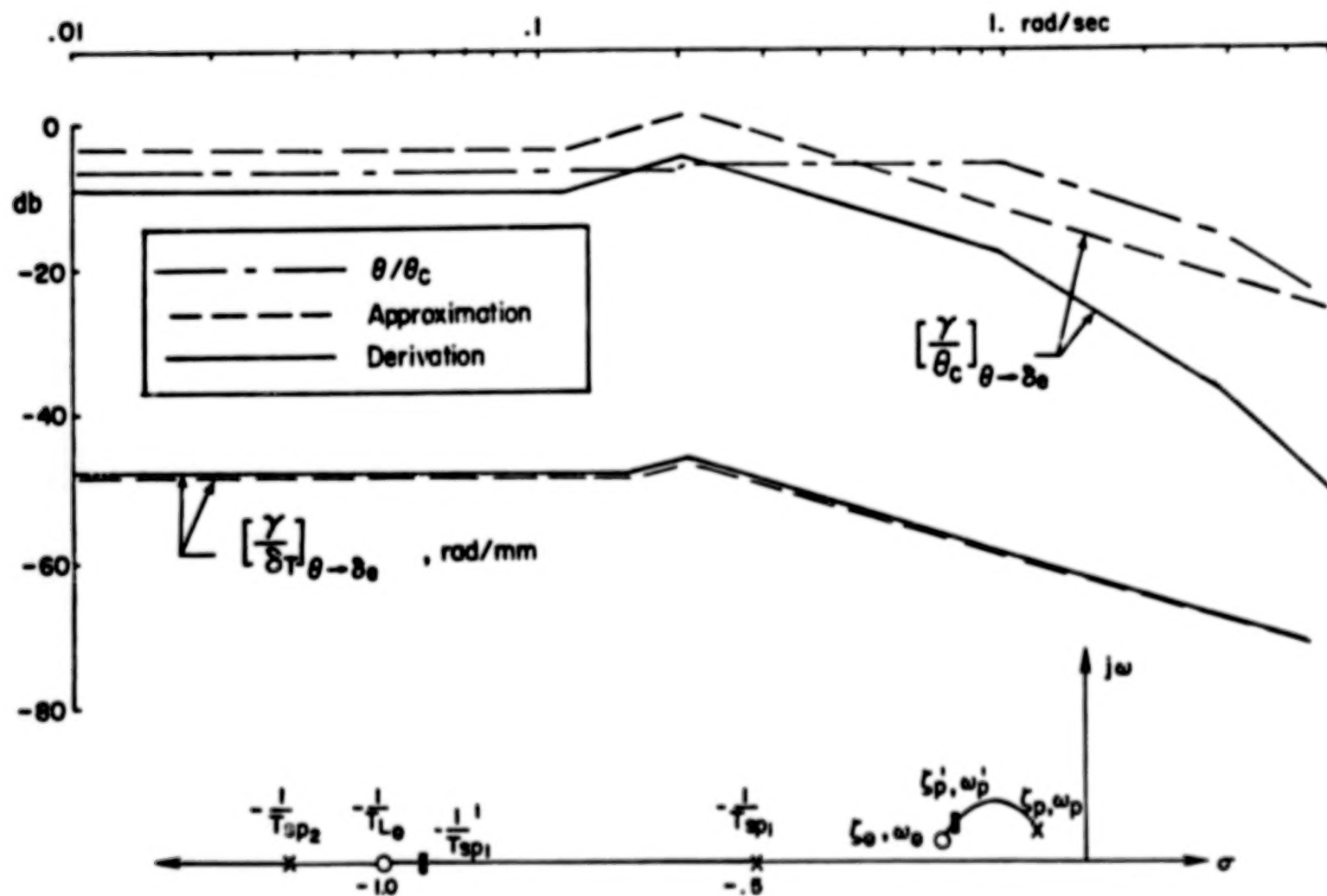


FIGURE 9b. TG4A: CLOSED LOOP FREQUENCY RESPONSE AND ROOT LOCUS

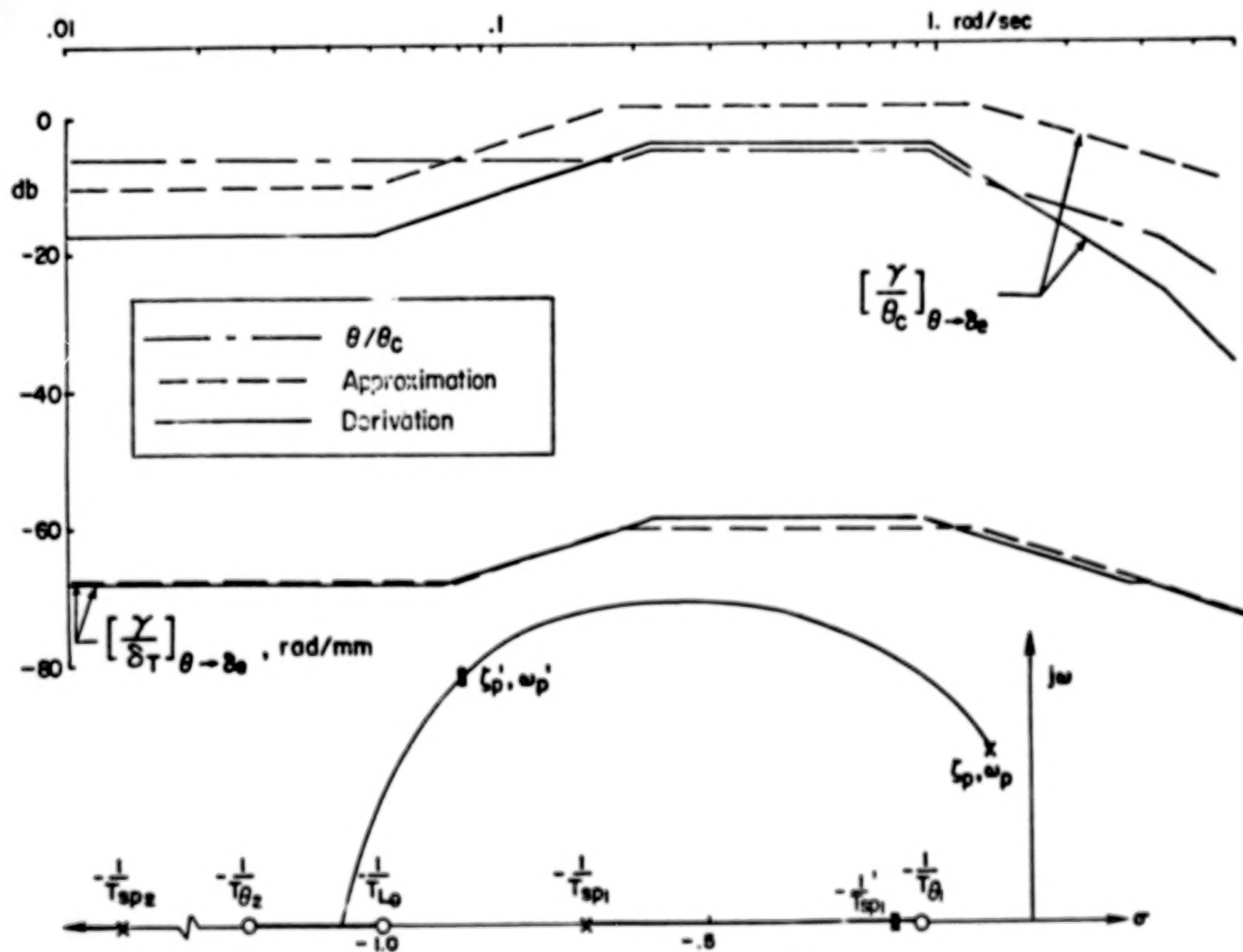


FIGURE 9c. TG1C: CLOSED LOOP FREQUENCY RESPONSE AND ROOT LOCUS

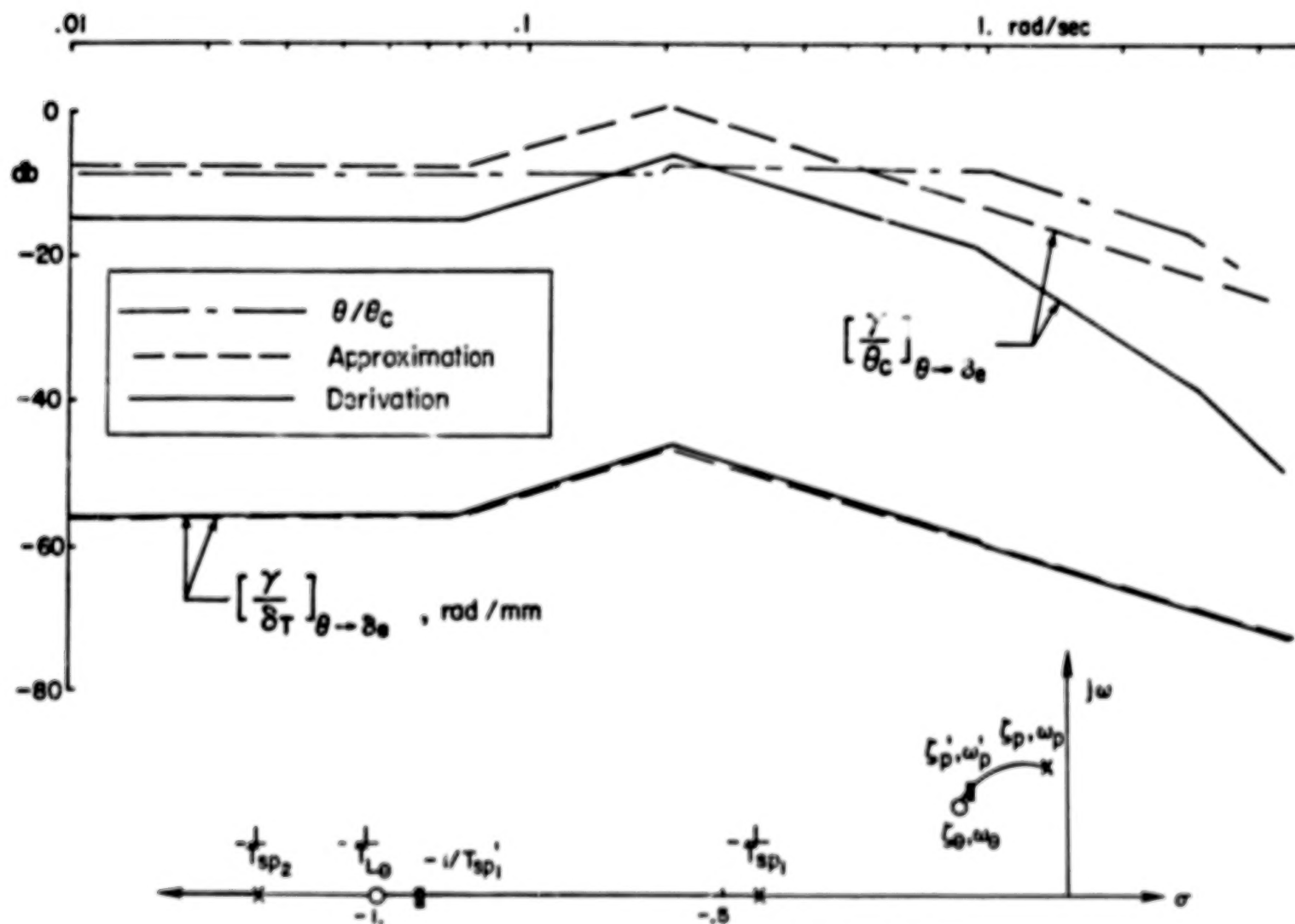


FIGURE 9d. TG3C: CLOSED LOOP FREQUENCY RESPONSE AND ROOT LOCUS

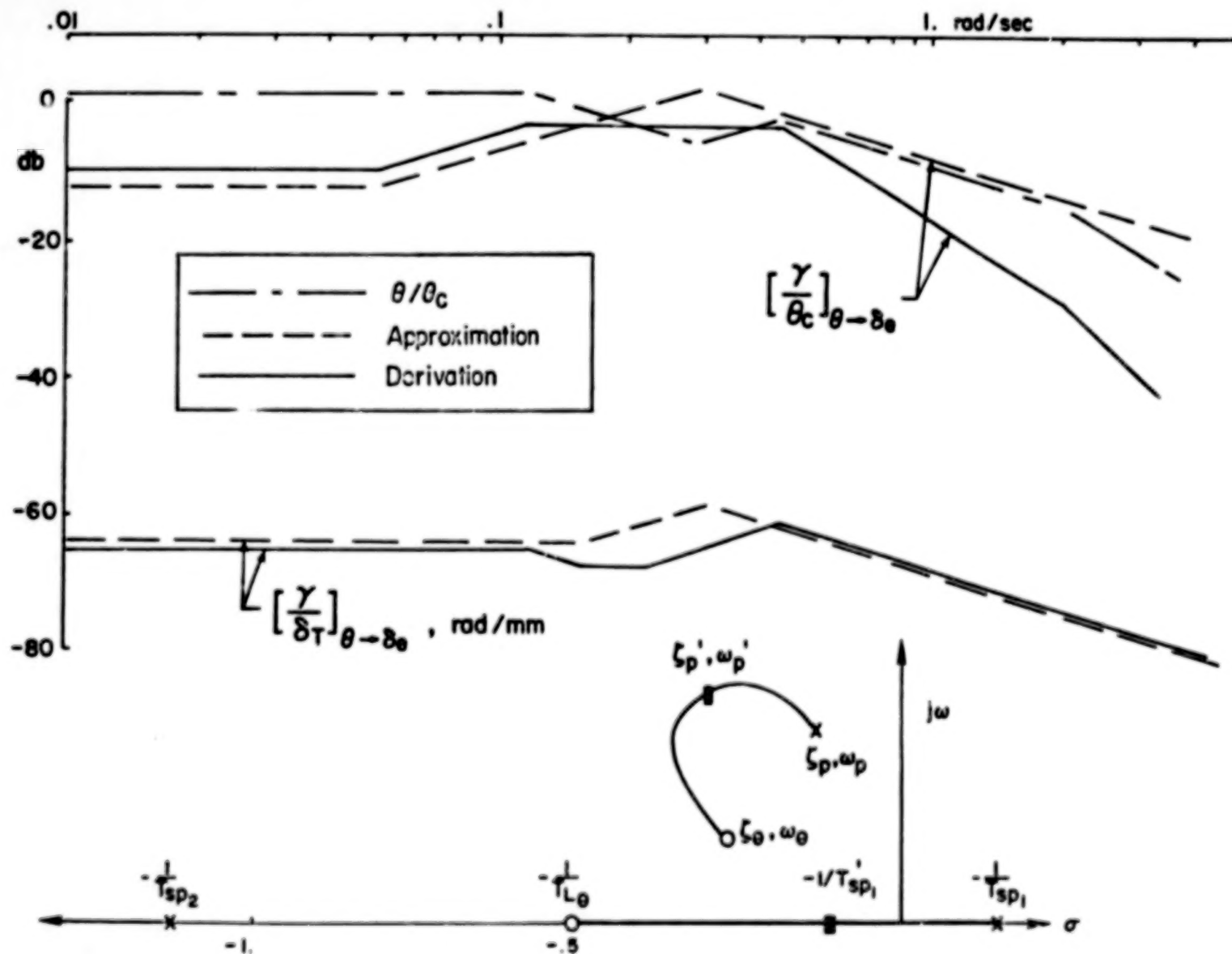


FIGURE 10a. BSL1, LOW GAIN SAS, NO $\frac{s+a}{s}$ OR τ_e

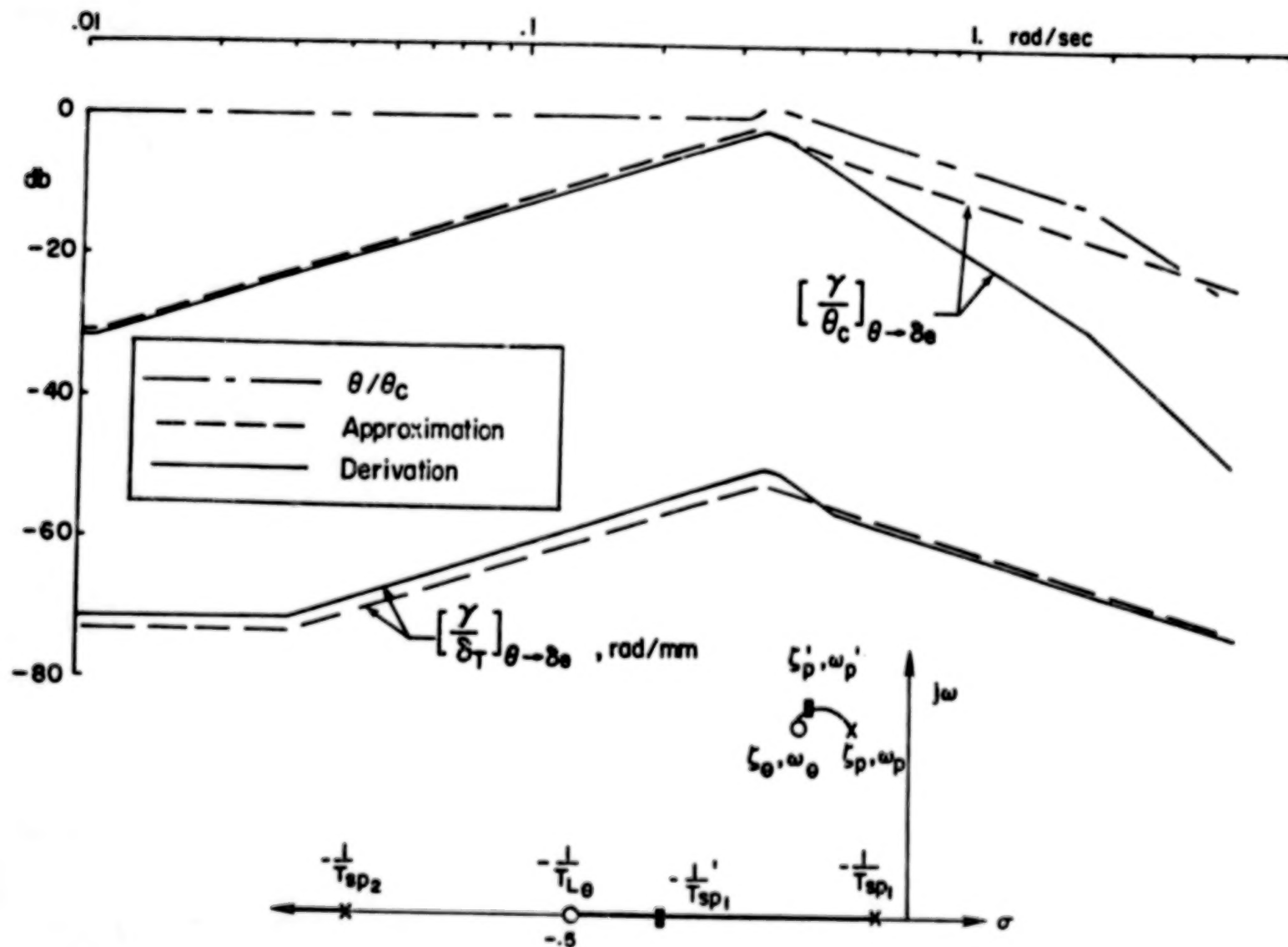


FIGURE 10b. AP1, LOW GAIN SAS, NO $\frac{s+a}{s}$ OR τ_e

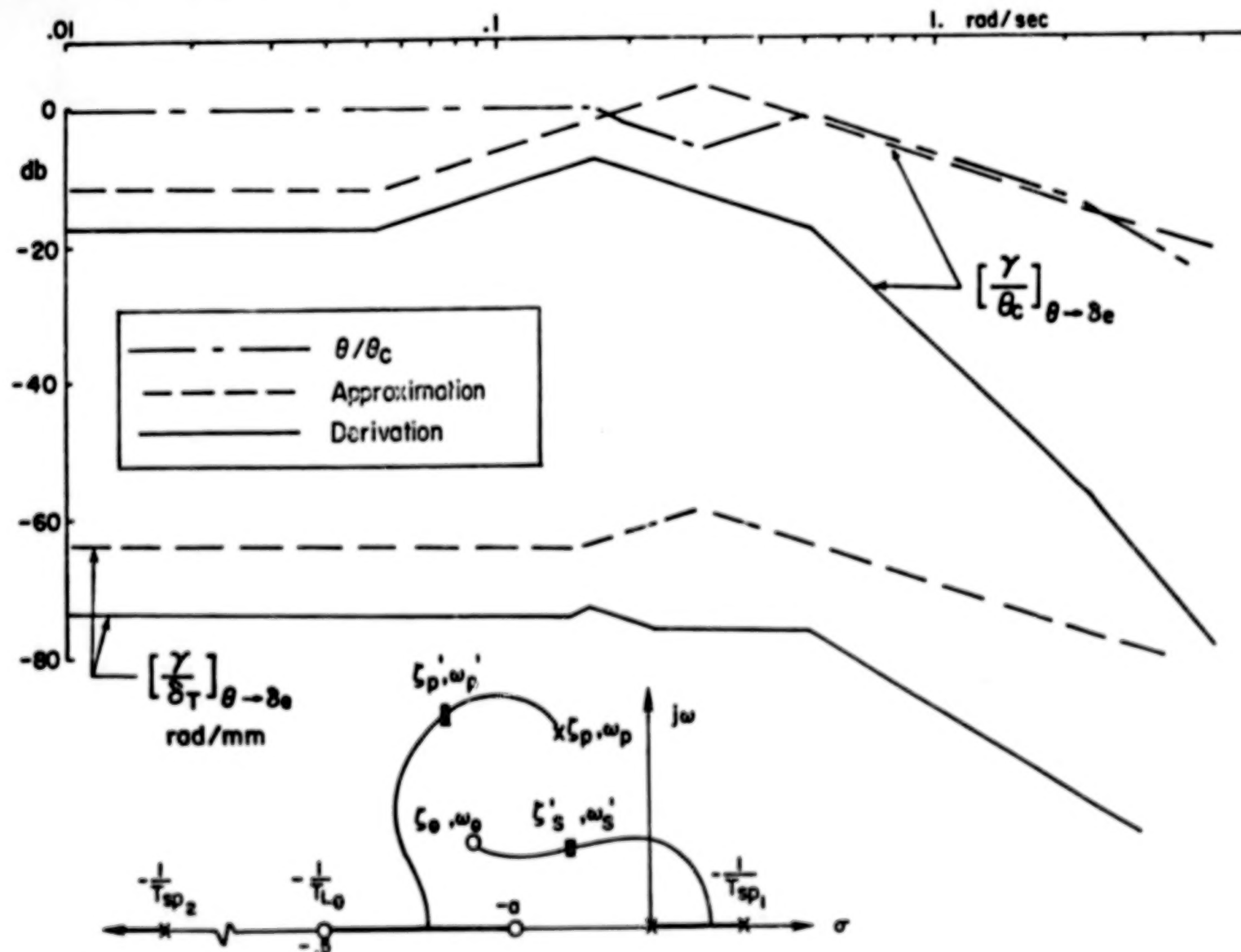


FIGURE 11a. BSL1, LOW GAIN, COMPLETE SAS

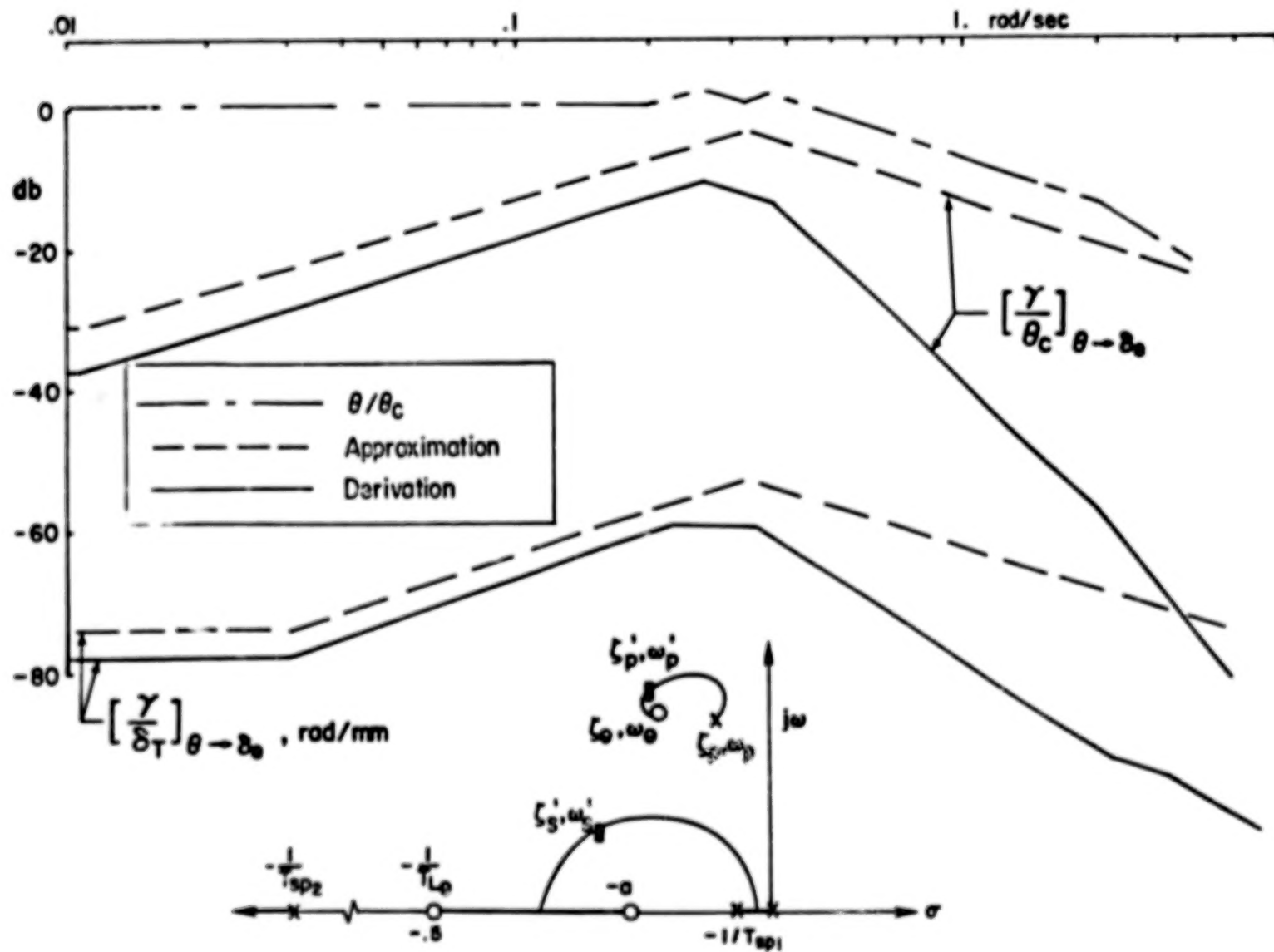


FIGURE 11b. AP1, LOW GAIN, COMPLETE SAS

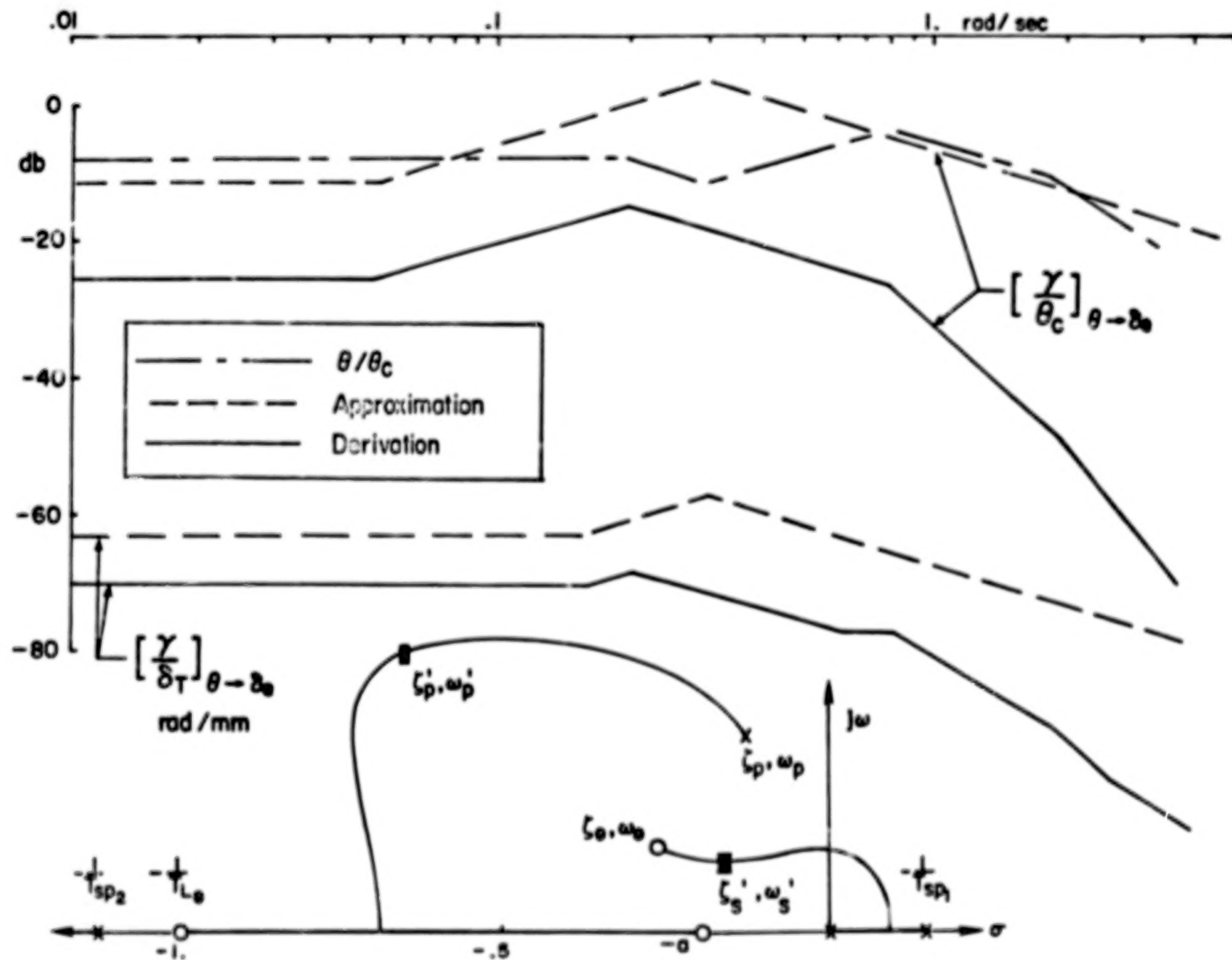


FIGURE 12a. BSL1, HIGH GAIN, COMPLETE SAS

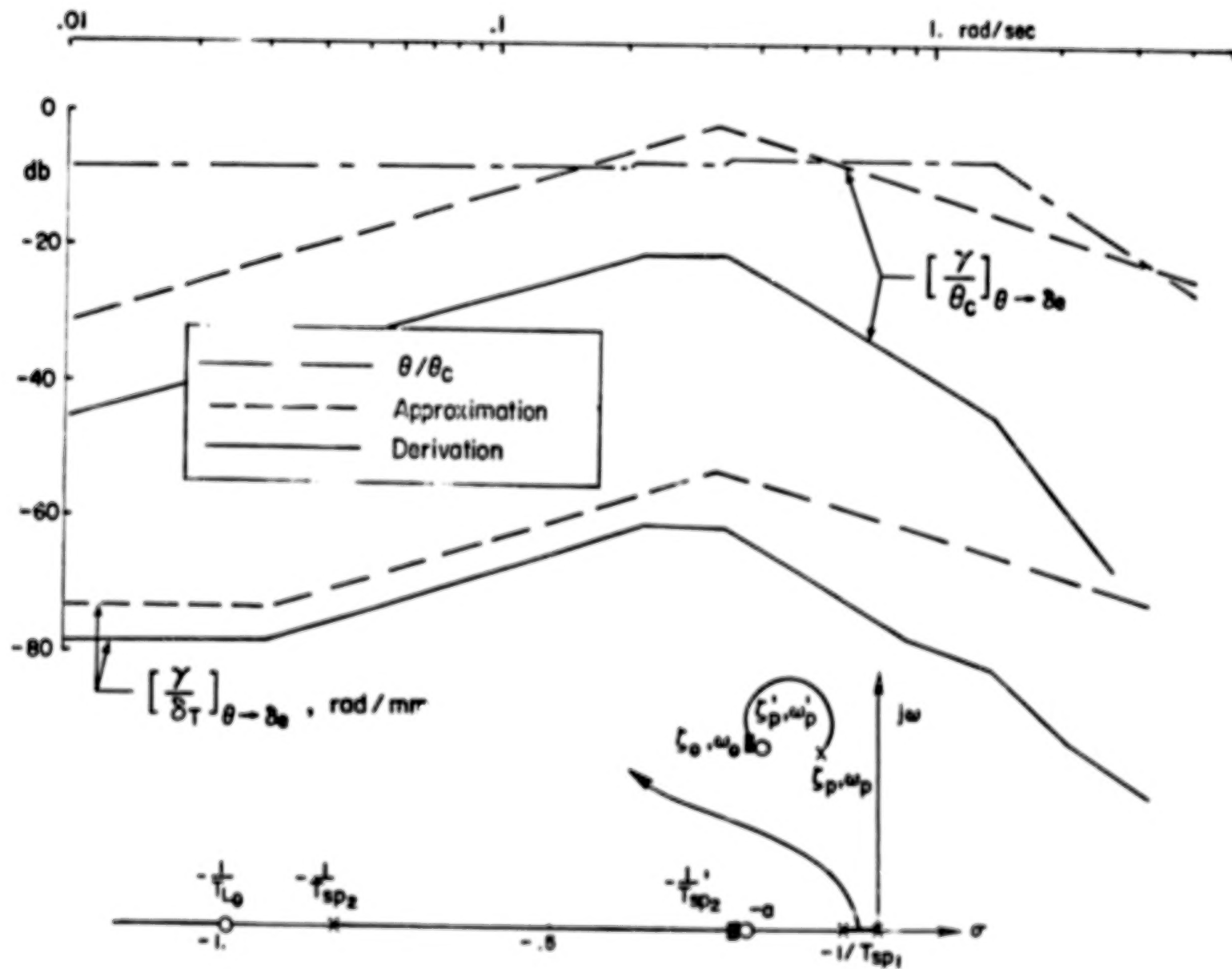


FIGURE 12b. AP1, HIGH GAIN, COMPLETE SAS

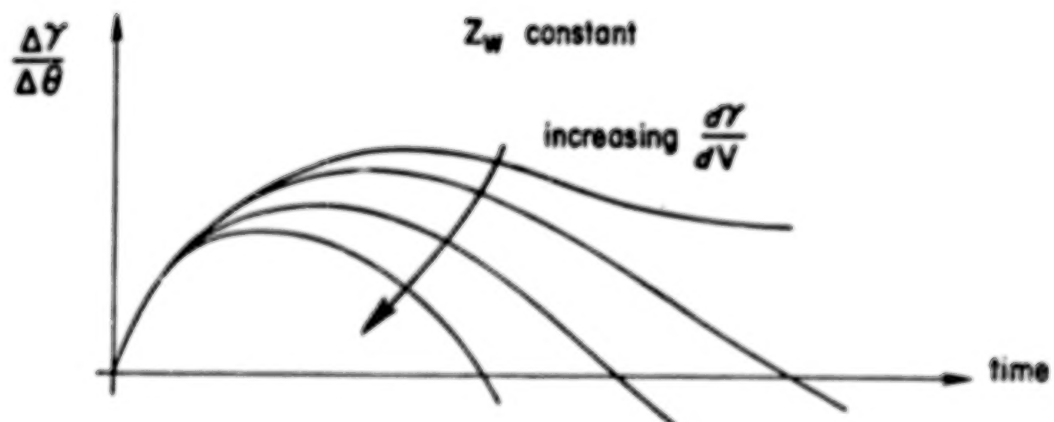


FIGURE 13a. EFFECT OF $\frac{d\gamma}{dV}$ ON STICK RESPONSE

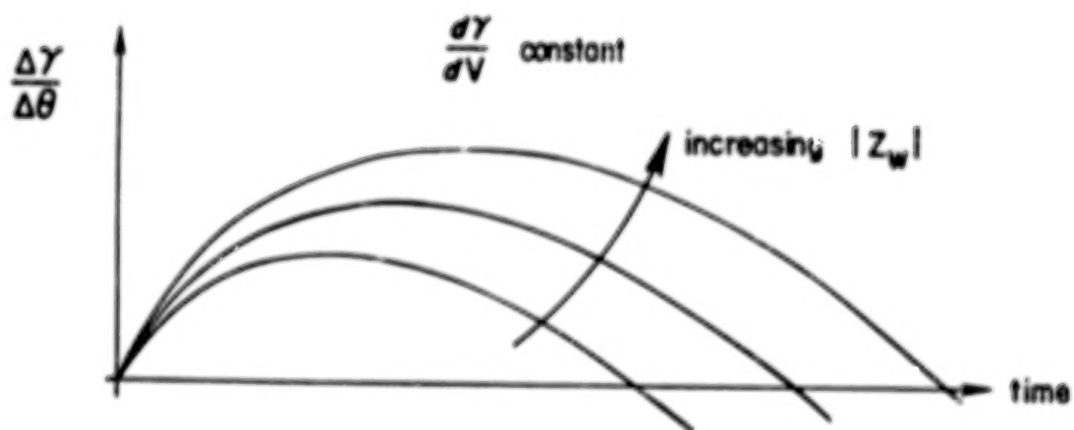


FIGURE 13b. EFFECT OF Z_w ON STICK RESPONSE

BLANK

PAGE

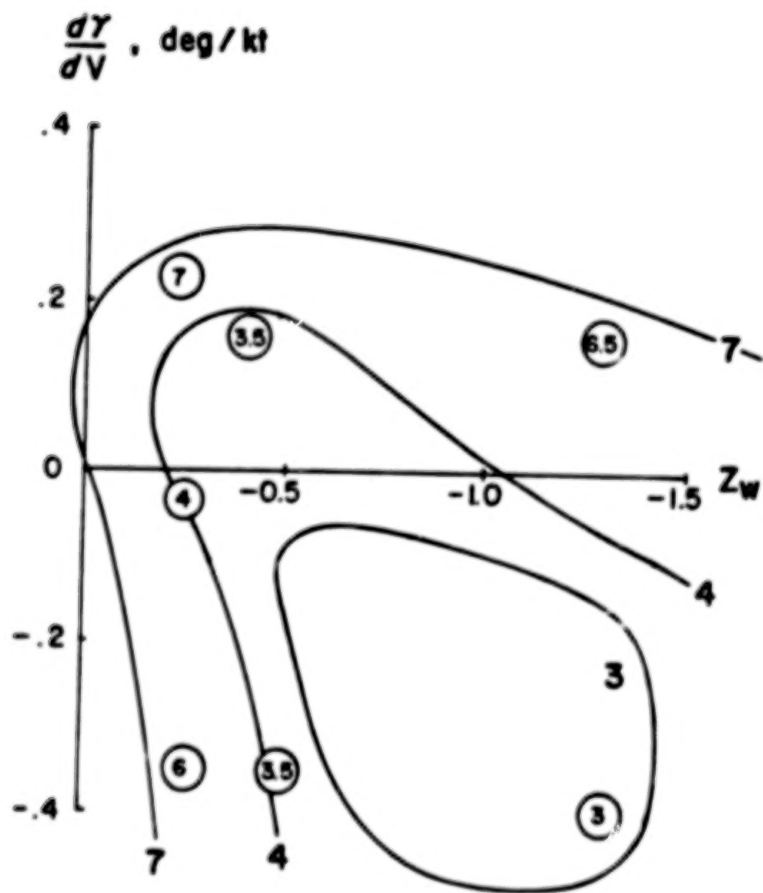
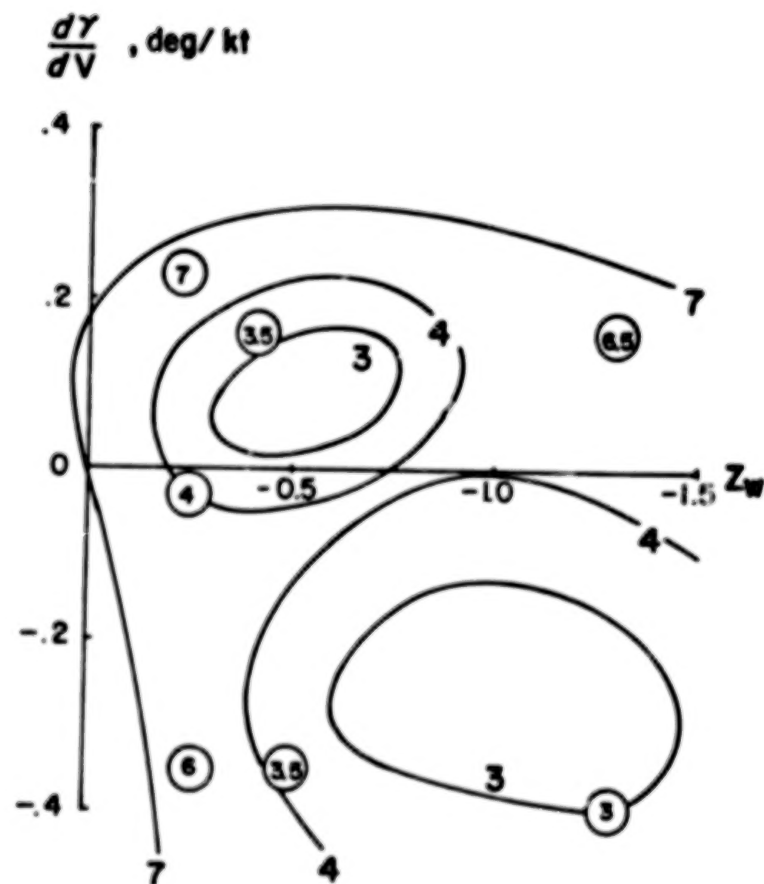
a.b.

FIGURE 14. POSSIBLE PILOT OPINION CONTOURS

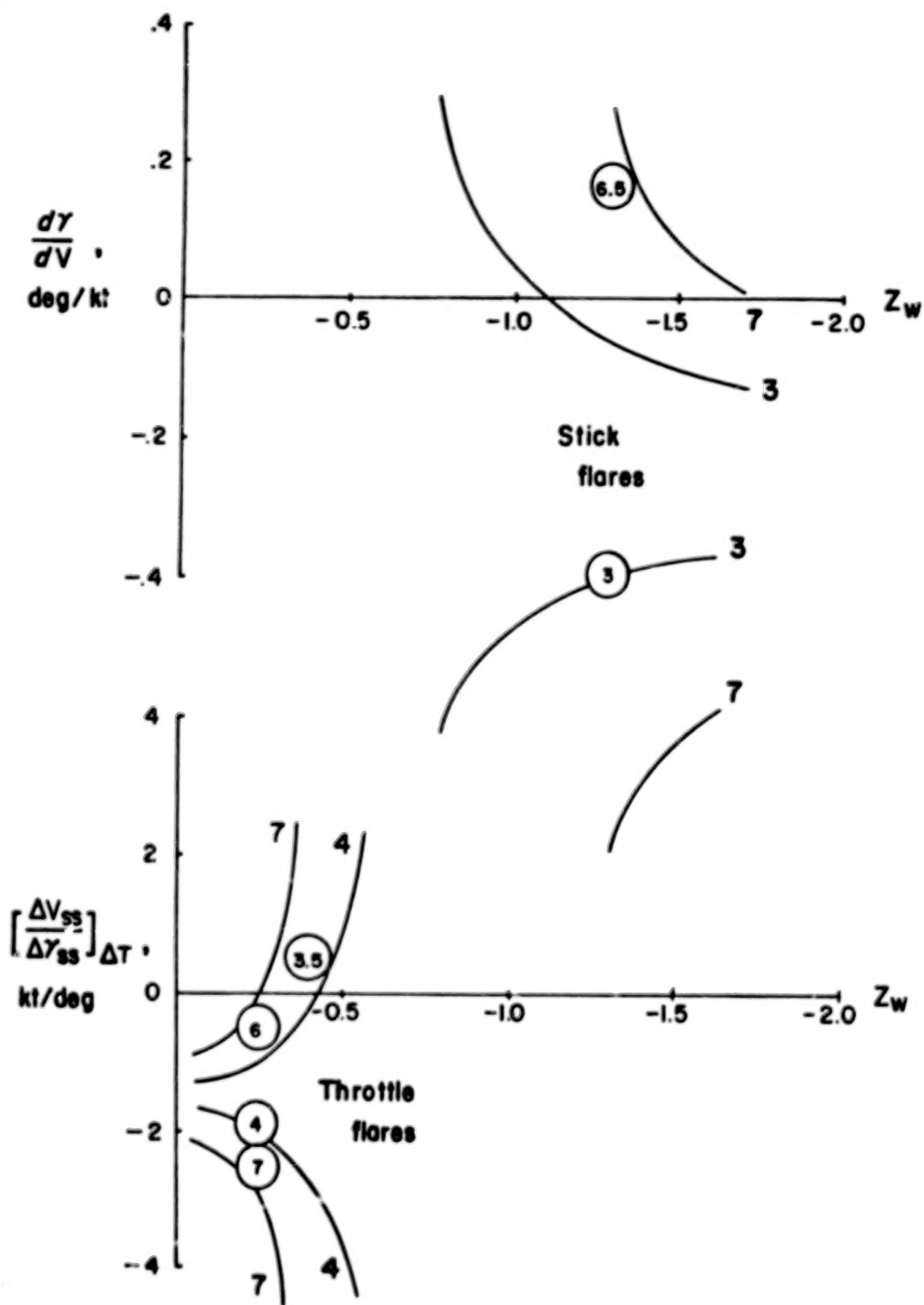


FIG. 14c

BLANK

PAGE

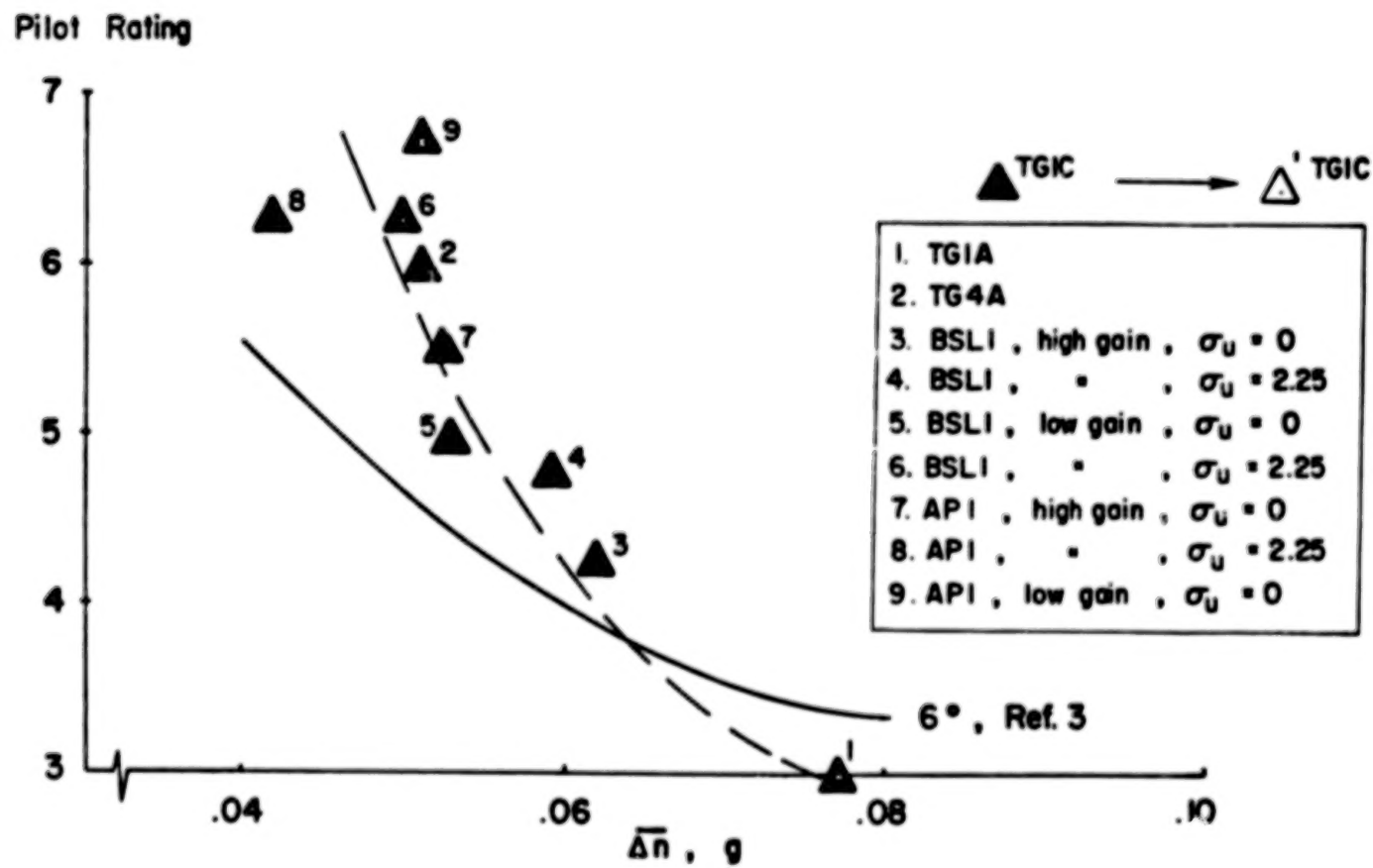


FIGURE 15. PILOT RATING vs. LOAD FACTOR

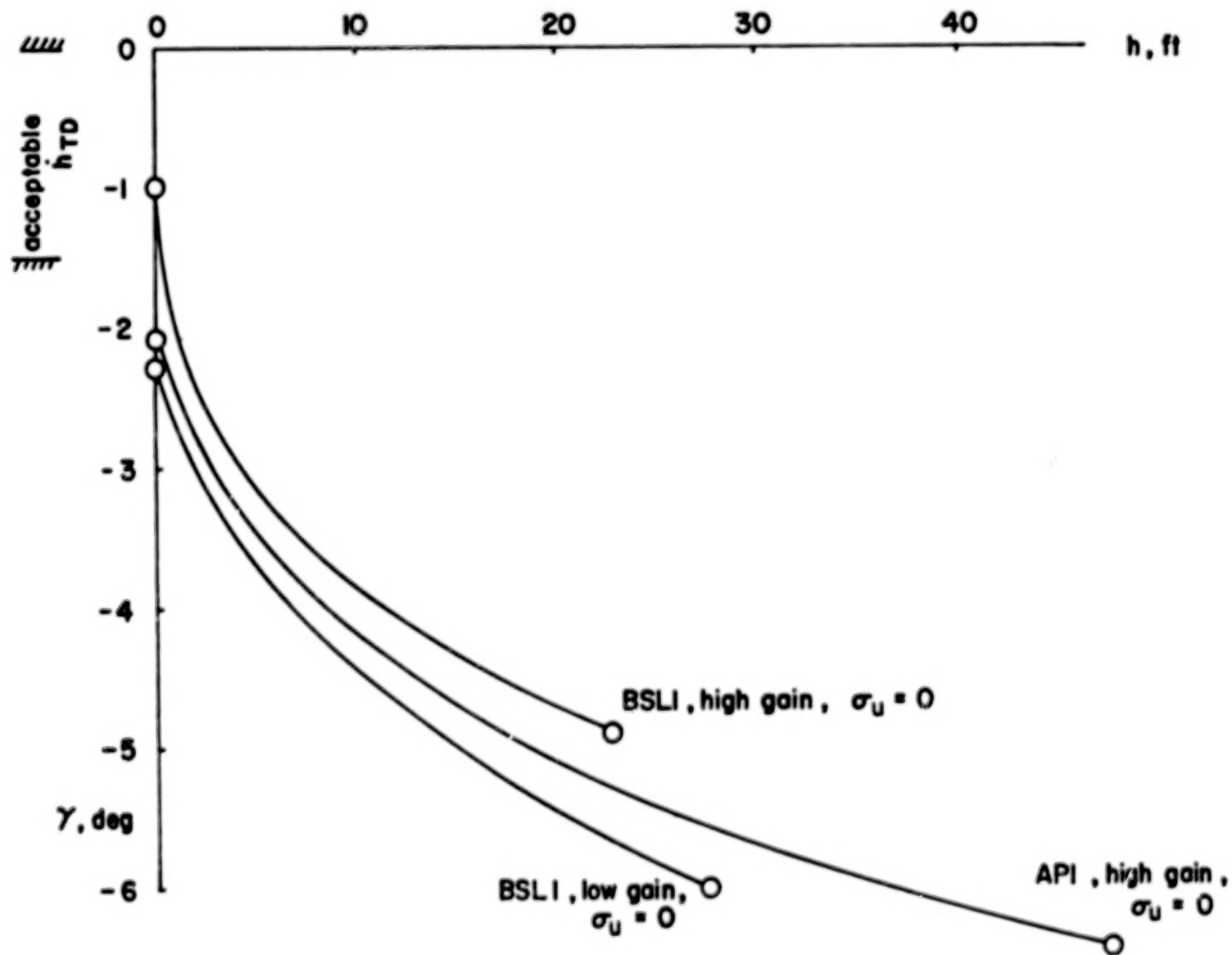


FIGURE 16. SOME h - γ TRAJECTORIES

1. Report No. NASA CR-3191		2. Government Accession No.		3. Recipient's Catalog No.	
4. Title and Subtitle An Exploratory Investigation of the STOL Landing Maneuver				5. Report Date December 1979	
				6. Performing Organization Code	
7. Author(s) Patrick H. Whyte				8. Performing Organization Report No. AMS 1231-T	
9. Performing Organization Name and Address Flight Research Laboratory Princeton University, James Forrestal Campus Princeton, N. J. 08544				10. Work Unit No.	
				11. Contract or Grant No. NAS2-7350	
12. Sponsoring Agency Name and Address Ames Research Center National Aeronautics and Space Administration Moffett Field, CA 94035				13. Type of Report and Period Covered Technical Report- Final	
				14. Sponsoring Agency Code	
15. Supplementary Notes					
16. Abstract <p>The parameters influencing the STOL landing are identified and their effect on the ease and quality of the flare maneuver is discussed. Data from actual landings, supported by pilot commentary and pilot opinion rating, are analyzed in order to gain an appreciation for the problem of performing an acceptable STOL landing.</p> <p>More flight testing is unquestionably required before conclusive results are available. Hypotheses concerning the prediction of STOL handling qualities in the flare are proposed, and suggestions put forward to direct future research along the most profitable course.</p>					
17. Key Words (Selected by Author(s)) Aircraft Flying Qualities, Atmospheric Flight Mechanics, STOL Aircraft, Approach and Landing, Flight Controls				18. Distribution Statement Unclassified-Unlimited STAR Category - 02	
19. Security Classif. (of this report) Unclassified		20. Security Classif. (of this page) Unclassified		21. No. of Pages 72	
				22. Price* \$5.25	

*For sale by the Clearinghouse for Federal Scientific and Technical Information, Springfield, Virginia 22151.

90%



END